AMERICAN SOCIETY FOR MICROBIOLOGY | Journal of Bacteriology®

RESEARCH ARTICLE

Comprehensive Spatial Analysis of the *Borrelia burgdorferi* Lipoproteome Reveals a Compartmentalization Bias toward the Bacterial Surface

Alexander S. Dowdell,[a] Maxwell D. Murphy,[a]* Christina Azodi,[a]* Selene K. Swanson,[b] Laurence Florens,[b] Shiyong Chen,[a,c] Wolfram R. Zückert[a]

Department of Microbiology, Molecular Genetics & Immunology, University of Kansas School of Medicine, Kansas City, Kansas, USA[a]; Proteomics Center, Stowers Institute for Medical Research, Kansas City, Missouri, USA[b]; School of Life Sciences, Qingdao Agricultural University, Shandong, China[c]

ABSTRACT The Lyme disease spirochete *Borrelia burgdorferi* is unique among bacteria in its large number of lipoproteins that are encoded by a small, exceptionally fragmented, and predominantly linear genome. Peripherally anchored in either the inner or outer membrane and facing either the periplasm or the external environment, these lipoproteins assume varied roles. A prominent subset of lipoproteins functioning as the apparent linchpins of the enzootic tick-vertebrate infection cycle have been explored as vaccine targets. Yet, most of the *B. burgdorferi* lipoproteome has remained uncharacterized. Here, we comprehensively and conclusively localize the *B. burgdorferi* lipoproteome by applying established protein localization assays to a newly generated epitope-tagged lipoprotein expression library and by validating the obtained individual protein localization results using a sensitive global mass spectrometry approach. The derived consensus localization data indicate that 86 of the 125 analyzed lipoproteins encoded by *B. burgdorferi* are secreted to the bacterial surface. Thirty-one of the remaining 39 periplasmic lipoproteins are retained in the inner membrane, with only 8 lipoproteins being anchored in the periplasmic leaflet of the outer membrane. The localization of 10 lipoproteins was further defined or revised, and 52 surface and 23 periplasmic lipoproteins were newly localized. Cross-referencing prior studies revealed that the borrelial surface lipoproteome contributing to the host-pathogen interface is encoded predominantly by plasmids. Conversely, periplasmic lipoproteins are encoded mainly by chromosomal loci. These studies close a gap in our understanding of the functional lipoproteome of an important human pathogen and set the stage for more in-depth studies of thus-far-neglected spirochetal lipoproteins.

IMPORTANCE The small and exceptionally fragmented genome of the Lyme disease spirochete *Borrelia burgdorferi* encodes over 120 lipoproteins. Studies in the field have predominantly focused on a relatively small number of surface lipoproteins that play important roles in the transmission and pathogenesis of this global human pathogen. Yet, a comprehensive spatial assessment of the entire borrelial lipoproteome has been missing. The current study newly identifies 52 surface and 23 periplasmic lipoproteins. Overall, two-thirds of the *B. burgdorferi* lipoproteins localize to the surface, while outer membrane lipoproteins facing the periplasm are rare. This analysis underscores the dominant contribution of lipoproteins to the spirochete's rather complex and adaptable host-pathogen interface, and it encourages further functional exploration of its lipoproteome.

KEYWORDS cell envelope, lipoproteins, localization, membrane biogenesis, membrane proteins, outer membrane, protein secretion, proteomics, spirochetes, surface proteins

Received 1 September 2016 **Accepted** 3 January 2017

Accepted manuscript posted online 9 January 2017

Citation Dowdell AS, Murphy MD, Azodi C, Swanson SK, Florens L, Chen S, Zückert WR. 2017. Comprehensive spatial analysis of the *Borrelia burgdorferi* lipoproteome reveals a compartmentalization bias toward the bacterial surface. J Bacteriol 199:e00658-16. https://doi.org/10.1128/JB.00658-16.

Editor Thomas J. Silhavy, Princeton University

Address correspondence to Shiyong Chen, shiyongchen@hotmail.com, or Wolfram R. Zückert, wzueckert@kumc.edu.

* Present address: Maxwell D. Murphy, Graduate Program in Bioengineering, University of Kansas, Lawrence, Kansas, USA; Christina Azodi, Graduate Program in Plant Biology, Michigan State University, East Lansing, Michigan, USA.

Bacterial lipoproteins are a class of membrane proteins that are peripherally anchored via an N-terminal lipid modification in the bacterial envelope, where they assume a variety of biological roles (reviewed in references 1–3). First translated as unmodified precursors in the cytoplasm, they are exported across the cytoplasmic membrane through recognition of an N-terminal signal peptide (4, 5). Export in an unfolded conformation occurs via the general secretory (Sec) pathway (6, 7), or less commonly after folding in the cytoplasm through the twin-arginine transport (TAT) pathway (8–12). In the periplasm, the lipoprotein precursor is posttranslationally modified by attachment of a diacylglycerol moiety to the sulfhydryl group of a conserved Cys residue, which is the first residue following the N-terminal signal peptide (13). The signal peptide is then removed by a specialized signal II/leader sequence peptidase (Lsp) (14), at which point the lipoprotein may be additionally modified by attachment of an acylglycerol to the now-free amine group of the new N-terminal cysteine by the Lnt enzyme (15–18). This final step is most common in Gram-negative bacteria and is uncommon in Gram-positive organisms (19, 20). In bacteria with a double-membrane (diderm) architecture, such as *Escherichia coli* or *Pseudomonas* spp., the mature lipoprotein can either be retained in the cytoplasmic inner membrane (IM) or exported to the outer membrane (OM), which is most frequently performed through the actions of the lipoprotein outer membrane localization (Lol) pathway (21–26).

Some Gram-negative bacteria express surface-exposed lipoproteins (27–45) but, with the exception of recently discovered surface lipoproteins in the phylum *Bacteroidetes* (43, 45), they remain relatively rare. In the Gram-negative model organism *E. coli*, only 7 of the about 90 expressed lipoproteins (46, 47) were detected on the bacterial surface but remained restricted to a proportion of total protein and certain protein domains, indicating rather complex and dynamic OM topologies (39, 42, 48–52).

Borrelia burgdorferi, the spirochetal agent of tick-borne Lyme borreliosis, has a diderm envelope architecture that is similar to but distinct from the one found in Gram-negative bacteria (53). By one estimate, about 8% of the genome of *B. burgdorferi* type strain B31 encodes 127 distinct potential lipoproteins (54). While studies have identified a wide gamut of biological functions for these lipoproteins, the early identification of major and immunodominant surface lipoproteins facilitating the enzootic cycle of Lyme borreliosis led to a focused effort to identify and characterize additional lipoproteins at the interface of the pathogen with its vector and host (55). This resulted in the identification, characterization, and localization of 49 lipoproteins, most of them being surface proteins (56–86) (Table 1).

Our own earlier work on lipoprotein sorting in *B. burgdorferi* showed that surface secretion signals of *Borrelia* surface lipoproteins were encoded within their disordered N-terminal tether peptides, but the analysis failed to identify any specific primary sequence motifs within wild-type tethers that would predict localization as the "+2/+3/+4" rule does for periplasmic lipoproteins in other eubacteria (87–90). Based on a large set of lipoprotein tether mutants (57, 76, 91–94), we concluded that the diverse surface lipoprotein tether peptides were essential for maintaining surface lipoproteins in a secretion-competent conformation, most likely by triggering protein-protein interactions with a periplasmic holding chaperone in a mechanism that could be similar to the high-affinity, low-specificity interaction of diverse signal peptides released from the ribosome with the cytoplasmic chaperone SecB (95–98). Yet, it remained entirely possible that spirochetal lipoprotein sorting motifs remained obscured by the rather limited and surface-biased data set of already-localized *B. burgdorferi* lipoproteins.

To remove this limitation in our data set and to gain a better understanding of a spirochetal cell envelope composition and structure, we therefore decided to further explore the spatial distribution of the *B. burgdorferi* lipoproteome. Using a library of epitope-tagged lipoproteins expressed by individual *B. burgdorferi* clones, we localized each lipoprotein to a distinct cellular compartment. We then validated our results using quantitative mass spectrometry of the endogenously *B. burgdorferi* lipoproteome expressed under standard culture conditions. Finally, we cross-referenced our results with existing data on the temporal expression and immunogenicity of *B. burgdorferi* proteins

TABLE 1 *B. burgdorferi* lipoproteome localization data[a]

ORF[b]	Protein name[c]	Localization[d]		dNSAF ratio[e]	Previous localization (reference)[f]	Molecular mass (kDa)		Paralogous family (no.)[g]	*In vivo* differential expression[h]	Immunogenicity[i]
		Consensus	His tag			Predicted	Observed			
BB0028		P-OM	S●	0.70	P-OM (56)	40	38			
BB0141	BesA	P-IM	P-IM	0.59		35	39			
BB0144	ProX	P-IM	P-IM	0.79		33	32			
BB0155		P-IM	P-IM	ND		44	41			
BB0158	S2	S	S	10.34		27	27	S2 (44)		
BB0171		S	S	ND		23	20			
BB0193		P-IM	P-IM	2.22		29	28			
BB0213		S	S	1.21		26	26			
BB0215	PstS	P-IM	P-IM	1.04		31	30			+
BB0224		P-IM	P-IM	ND		11	12			
BB0227		P-IM	P-IM	0.57	P-OM (57)	27	26			
BB0298		P-IM	P-IM	0.37	P (58)	26	26			
BB0323		P-OM	P-IM	0.47	P-OM (59)	44	14			+
BB0324		P-OM	P-OM	0.69	P-OM (56)	14	16			
BB0328	OppA1	P-IM	P-IM	0.57	S (60)	60	59	OppA (37)		+
BB0329	OppA2	P-IM	P-IM	0.94	S (61)	61	60	OppA (37)		+
BB0330	OppA3	P-IM	P-IM	0.92		62	57	OppA (37)		
BB0352		S	S	ND		44	39			
BB0365	IpLA7	P-IM	P-IM	0.57	P-IM (62)	22	21		TA, TP	+
BB0382	BmpB	P-IM	P-IM	1.16	S (63)	38	34	Bmp (36)		
BB0384	BmpC	P-IM	P-IM	0.45		40	39	Bmp (36)		
BB0385	BmpD	P-IM	P-IM	0.89		37	38	Bmp (36)		+
BB0398		P-IM	P-IM	0.00		41	36			
BB0456		P-IM	P-IM	0.12		24	23			
BB0460		P-OM	P-OM	2.02		28	29		VT, VP	
BB0475		P-OM	P-OM	ND		15	13			
BB0536		ND	ND	0.67		108	ND			
BB0542		P-IM	P-IM	1.26		22	19		VT	
BB0628		P-IM	P-IM	0.00		27	26			
BB0652	SecD	P-IM	ND	0.18		65	ND			+
BB0664		P-IM	P-IM	0.70		26	28			
BB0689		S	S	19.87	S (58)	18	17		VT	
BB0758		S	S	ND		25	26		VP	
BB0806		P-IM	P-IM	1.22		58	53			
BB0823		S	S	ND		14	17		VP	
BB0832		P-IM	P-IM	0.73		31	27			
BB0844		P-IM	P-IM	ND		37	38	BB0884 (12)	VP	+
BBA03		P-IM	P-IM	0.70	S (64)	19	17			+
BBA04	S2	S	S	∞		32	33	S2 (44)	VT	+
BBA05	S1	P-IM	P-IM	1.83	P (65)	49	52			
BBA07	ChpAI	S	S	∞	S (66)	18	21		VT	+
BBA14		S	S●	0.63		14	14	OrfD (143)	VP	
BBA15	OspA	S	S	65.42	S (67)	29	31	OspAB (53)	TA, TP	+
BBA16	OspB	S	S	185.84	S (68)	32	34	OspAB (53)	TA, TP, VT	+
BBA24	DbpA	S	S	5.95	S (69)	21	21		VT, VP	
BBA32		S	S	ND		8	13			
BBA33		S	S	ND	S (70)	21	19		VP	
BBA34	OppA5	P-IM	P-IM	0.74	P (71)	61	59	OppA (37)	VP	+
BBA36		S	S	ND	S (58)	24	23		VP	+
BBA57		S	S	0.62	S (72)	47	56		VP	+
BBA59		S	S	2.93		9	18		TA, TP, VT	
BBA62	Lp6.6	P-OM	P-OM	0.59	P-OM (73)	8	13		TA, TP, VT	
BBA64	P35	S	S	6.23	S (58)	34	32	P35 (54)		+
BBA65		S	S●	ND	S (74)	32	26	P35 (54)		
BBA68	CspA	S	S	24.36	S (75)	29	27	P35 (54)		
BBA69		S	S	∞	S (58)	30	31	P35 (54)	VP	
BBA72		P-IM	P-IM	ND		9	13			
BBB08		S	S	0.61		25	27			
BBB09		P-OM	P-OM	ND		41	36		VT	+
BBB16	OppA4	P-IM	P-IM	0.61	P-IM (76)	61	58	OppA (37)		+
BBB19	OspC	S	S	7.86	S (77)	22	22		VT	+

(Continued on following page)

TABLE 1 (Continued)

ORF[b]	Protein name[c]	Localization[d]		dNSAF ratio[e]	Previous localization (reference)[f]	Molecular mass (kDa)		Paralogous family (no.)[g]	*In vivo* differential expression[h]	Immunogenicity[i]
		Consensus	His tag			Predicted	Observed			
BBB25		S	S●	0.52		19	18		VP	
BBB27		P-IM	P-IM	1.25	P-OM (57)	22	21			
BBC10	RevB	S	S	ND		20	19	Rev (63)		+
BBD10		S	S	1.83		23	21			
BBE04		S	S	ND		5	13	54		
BBE08		S	S	ND		6	8			
BBE31	P35	S	S	∞	S (78)	28	27	P35 (60)	VT	
BBF01	ErpD	S	S	ND		37	50	ErpB (163)		
BBF20		S	S	1.84		11	14			
BBG01		S	S	73.49		35	31	BB0884 (12)	VP	
BBG25		P-OM	P-OM	ND		15	15	OrfD (143)	VP	
BBH01		S	S	ND		8	13	BBH01 (166)	VP	
BBH06	CspZ	S	S●	0.74	S (79)	27	26	CRASP-2	VP	+
BBH18		S	S	5.94		43	43			
BBH32	P35	S	S	8.36		29	22	P35 (60)		
BBH37		S	S	62.20		33	37	BB0884 (12)	VP	
BBI14		S	S	ND		4	8	60	VP	
BBI16	VraA	S	S	∞	S (80)	54	75	P35 (60)		
BBI28		S	S	ND		22	21	P35 (60)	VP	
BBI29		S	S	8.94		26	27	P35 (60)	TA, TP, VT	
BBI36	P35	S	S	85.93		32	37	P35 (54)		
BBI38		S	S	0.00		32	38	P35 (54)	VP	
BBI39		S	S	56.21		33	37	P35 (54)	VP	
BBI42		S	S	ND	S (58)	21	20	BBI42 (52)	VP	+
BBJ01		S	S	ND		7	11	P35 (60)		
BBJ09	OspD	S	S	22.89	S (81)	28	29		VP	
BBJ34		S	S	142.70		40	41	CRASP-2 (92)	VP	
BBJ36		S	S	∞		40	35	CRASP-2 (92)		
BBJ41	P35	S	S	ND		33	37	P35 (54)	VP	
BBJ47		P-IM	P-IM	ND		27	26			
BBK01		S	S	97.29		34	38	BB0884 (12)	VP	
BBK07		S	S	∞	S (82)	28	31	BBK07 (59)		+
BBK12		S	S	ND		26	31	BBK07 (59)		+
BBK19		S	S	39.92		24	30			+
BBK32	Fbp	S	S	ND	S (83)	41	48			+
BBK48	P37	S	S	ND		33	40	P37 (75)		
BBK50	P37	S	S	10.42		37	46	P37 (75)		
BBK52	P23	S	S	ND		33	30	S2 (44)		+
BBK53		S	S	ND		21	20	BBI42 (52)	VT	+
BBL28	MlpH	S	S	∞		17	19	Mlp (113)		
BBL39*	ErpN	S	S	10.87	S (84)	20	19	ErpA (162)		+
BBL40*	ErpO	S	S	1.03	S (84)	44	ND	ErpB (163)	VT	+
BBM27*	RevA1	S	S	0.93	S (85)	18	ND	Rev (63)	VP	+
BBM28	MlpF	S	S	ND		17	15	Mlp (113)		
BBM38	ErpK	S	S	ND	S (84)	29	37	ErpG (164)		
BBN28	MlpI	S	S	ND		16	18	Mlp (113)	VP	+
BBN38	ErpP	S	S	38.48	S (84)	21	20	ErpA (162)		+
BBN39	ErpQ	S	S	∞	S (84)	39	55	ErpB (163)		+
BBO28	MlpG	S	S	ND		16	16	Mlp (113)		
BBO39	ErpL	S	S	ND	S (84)	26	29	ErpG (164)		+
BBO40	ErpM	S	S	0.61	S (84)	42	40	ErpB (163)		+
BBP27	RevA2	S	S	0.93	S (85)	18	18	Rev (63)	VP	
BBP28	MlpA	S	S	3.16		16	19	Mlp (113)	VP	
BBP38	ErpA	S	S	10.87	S (84)	20	18	ErpA (162)		
BBP39	ErpB	S	S	1.03	S (84)	44	61	ErpB (163)	VP	+
BBQ03		S	S	ND		21	19	BBI42 (52)	VP	+
BBQ05	P35	S	S	1.22		29	30	P35 (60)	VP	
BBQ35	MlpJ	S	S	1.83		24	21	Mlp (113)		+
BBQ46		ND	ND	ND		4	ND			
BBQ47	ErpX	S	S●	ND	S (84)	40	28	ErpB (163)	VP	
BBQ89*		S	S	ND		8	11	BBH01 (166)		

(Continued on following page)

TABLE 1 (Continued)

ORF[b]	Protein name[c]	Localization[d]		dNSAF ratio[e]	Previous localization (reference)[f]	Molecular mass (kDa)		Paralogous family (no.)[g]	*In vivo* differential expression[h]	Immunogenicity[i]
		Consensus	His tag			Predicted	Observed			
BBR28	MlpD	S	S	1.06		16	16	Mlp (113)	VP	
BBR40	ErpH	S	S	ND		4	9	162	VP	
BBR42	ErpY	S	S	∞	S (84)	25	27	ErpG (164)	VP	+
BBS30	MlpC	S	S	6.55		17	16	Mlp (113)		+
BBS41	ErpG	S	S	∞	S (86)	22	23	ErpG (164)	VP	+

[a]Localization data from the current study were reconciled with previously published data and data from genome-wide studies of *in vivo* gene expression, protein immunogenicity, and requirement for *in vitro* growth. A Microsoft Excel version of this table is available upon request.
[b]Open reading frame (ORF) for assayed lipoprotein (100, 101). *, ORFs that were identical in mature sequence to other analyzed ORFs (Fig. 1; see also the text).
[c]Common protein name used in the literature.
[d]Consensus, determined consensus localization of the assayed lipoproteins, as described in the text. S, surface; P-OM, periplasmic outer membrane; P-IM, periplasmic inner membrane; ND, not determined. His tag, determined localization of the C-terminally His-tagged proteins (Fig. 1 to 3). Localizations followed with a dot indicate that the His-tagged protein was resistant to proteinase K (Fig. 1) but not pronase (Fig. 3).
[e]dNSAF ratio ($dNSAF_{-pK}/dNSAF_{+pK}$) determined by MudPIT analysis (see the text). ∞, infinite value due to lack of detection of any peptides after pK treatment, i.e., division by 0.
[f]Previously determined and published lipoprotein localization.
[g]Paralogous family (represented by the key member) and number according to Casjens et al. (101).
[h]Observed *in vivo* expression pattern according to Iyer et al. (126). Transcripts that showed significant elevation in the fed larval stage relative to at least one other stage were classified as important for tick acquisition (TA) and/or tick persistence (TP), as the corresponding genes were upregulated in the transition from infected mice to naive larvae. Transcripts that showed significant elevation in the fed nymph stage relative to at least one other stage were associated with vertebrate transmission (VT), based on their apparent importance for the spirochete's passage from the feeding nymph to the naive mouse. Finally, transcripts that were significantly elevated in dialysis membrane chambers (DMCs) relative to at least one other stage were considered necessary for vertebrate persistence (VP), given their induction in a quasi-steady-state mammalian environment.
[i]Protein immunogenicity as determined by Barbour et al. (125).

to provide a basis for further studies in microbial pathogenesis, lipoprotein structure-function, and vaccine development.

RESULTS

Generation of an epitope-tagged lipoprotein expression library in *B. burgdorferi*. Our long-standing interest in understanding the biogenesis of spirochetal envelopes, particularly the sorting mechanisms for the numerous and abundant *B. burgdorferi* lipoproteins (1, 57, 76, 91–94, 99), has been continually thwarted by the quite limited and biased data set of characterized lipoproteins. As shown in Table 1, 49 *B. burgdorferi* lipoproteins have been localized independently to date, with over two-thirds of them found on the bacterial surface. We therefore set out to comprehensively localize the published list of proteins that are predicted to make up the *B. burgdorferi* lipoproteome (54). This list was compiled by training a computer algorithm (SpLip) on a set of spirochetal proteins that had been experimentally verified to be lipidated, and then using that trained algorithm to scan the published genome of *B. burgdorferi* B31 (100, 101). A total of 127 putative open reading frames (ORFs) were annotated as probable, possible, or false-negative lipoproteins (54). These 127 ORFs were used as our working lipoproteome for the creation of a C-terminally histidine-tagged expression library. This approach allowed us to use a single commercial blotting reagent (HisProbe-HRP) (HRP, horseradish peroxidase) to probe the entire lipoprotein library, bypassing the need to generate individual and validated lipoprotein-specific antibodies.

B. burgdorferi B31-e2 clones expressing each individual epitope-tagged lipoprotein were obtained as described in Materials and Methods. Of the 127 lipoproteins that were to be cloned, three (BB0536, BB0652 [SecD], and BBQ46) showed no expression of His-tagged protein in multiple *B. burgdorferi* clones; all clones contained the respective recombinant plasmid when assayed by PCR and DNA sequencing, indicating that the lack of expression was not due to absence of plasmid or mutation of the promoter or coding sequence. These three ORFs were not pursued further. In addition, four pairs of lipoproteins were found to be 100% identical in their mature processed sequences when analyzed by sequence alignment (T-Coffee [http://www.tcoffee.org/]) (102): BBP38 (ErpA) and BBL39 (ErpN), BBP39 (ErpB) and BBL40 (ErpO), BBP27 (RevA) and BBM27 (RevA), and BBH01 and BBQ89. As it is all but certain that proteins with identical

primary sequences localize identically (1), each of these pairs is represented by a single member (the first ORF listed of the pair). This resulted in an assayed data set of 120 unique lipoproteins covering 124 members (or 98%) of the predicted *B. burgdorferi* lipoproteome.

Initial assignment of lipoproteins to the bacterial surface based on proteinase K accessibility. We used an established and validated stepwise experimental protocol to individually localize each epitope-tagged lipoprotein within the spirochetal cell envelope. As described, we first subjected each recombinant *B. burgdorferi* clone to *in situ* surface proteolysis (or "proteolytic shaving") with proteinase K (pK), a membrane-impermeable nonspecific protease that selectively digests surface lipoproteins in the context of an intact OM (57, 76, 94). Surface lipoprotein OspA was used as a positive control, as it is readily degraded by proteinase K under the assay conditions. Conversely, the periplasmic flagellar protein FlaB was used as a negative control to ascertain OM integrity of the assayed cells. The His tag epitope was used to assess the sensitivity of the tagged lipoprotein to proteinase K, assuming that the localization of the C-terminal His tag mirrors that of the lipoprotein itself. Of note, C-terminal processing of secreted proteins in *B. burgdorferi* is rather specific and limited to a small set of proteins (103, 104), and C-terminal tags are not known to alter lipoprotein localization (57, 105). Lipoproteins that lost the His tag signal upon proteolysis were considered to be surface exposed (S), whereas lipoproteins that showed no loss in signal relative to the controls were considered to localize to the periplasmic (P) face of the OM or inner membrane (IM). Compiled Western blotting results for each of the assayed lipoproteins are shown in Fig. 1, organized by ascending ORF nomenclature. Of the 124 lipoproteins covered by the analysis, 83 lipoproteins were classified as surface exposed, while 41 lipoproteins were considered to localize to the periplasm. Interestingly, a subset of lipoproteins exemplified by the Mlp protein family showed only partial degradation of the His tag after proteinase K treatment (Fig. 1). This could indicate that only fractions of these lipoproteins are exported to the surface. Alternatively, it could reflect the lipoproteins' native folding, which may render their C termini less accessible to protease in the context of the spirochetal envelope.

Initial assignment of periplasmic lipoproteins to the outer or inner membrane by membrane fractionation. Recombinant *B. burgdorferi* clones that expressed epitope-tagged lipoproteins protected from surface proteolysis with proteinase K were subjected to membrane fractionation. OM vesicles (OMVs) and protoplasmic cylinder (PC) fractions were obtained as described in Materials and Methods by incubating harvested cells in a hypotonic citrate buffer, followed by loading on a stepwise sucrose gradient. Note that due to the not entirely efficient separation of the OM during the process (106), the PC fraction should be interpreted as a partially OM-depleted whole-cell protein fraction. Thus, the surface/OM control OspA is abundant in the OMV fractions but also detected in the PC fractions (57, 76). In contrast, the inner membrane lipoprotein OppAIV can be used as a control to assess the purity of the OMV preparation, as it should be absent from an ideal OMV preparation. A lipoprotein was scored as an OM component if the His tag was detected in the OMV fraction in a ratio similar to the OspA control. Absence or only traces of a His tag signal from the OMV fraction indicated that the lipoprotein was retained in the inner membrane. As shown in the Western immunoblots in Fig. 2, 31 of the 40 lipoproteins assayed showed an OppAIV-like fractionation pattern, i.e., they were retained in the IM. Conversely, 9 lipoproteins were detected in appreciable amounts in the OMV fraction, indicating that they were released to the OM.

Reassessment of select OM lipoproteins for potential intrinsic proteinase K resistance. The lipoprotein BBQ47 (ErpX) was previously established as a surface-exposed but intrinsically proteinase K-resistant protein (84). Consequently, the ErpX-expressing *B. burgdorferi* clone was not subjected to membrane fractionation despite the protein's apparent resistance to proteinase K. Yet, this example raised the specter that other surface lipoproteins may have been erroneously scored as OM periplasmic lipoproteins due to their resistance to proteinase K. We therefore reevaluated the 9 lipoproteins in our initial periplasmic OM (P-OM) lipoprotein data set using pronase, a


BB0028 BesA/AcrA BB0141 ProX BB0144 BB0155 S2 BB0158 BB0171 BB0193 BB0213 PstS BB0215 BB0224 BB0227 BB0298 BB0323
BB0324 OppA1 BB0328 OppA2 BB0329 OppA3 BB0330 BB0352 IpLA7 BB0365 BmpB BB0382 BmpC BB0384 BmpD BB0385 BB0398 BB0456 BB0460 BB0475
BB0536 BB0542 BB0628 SecD BB0652 BB0664 BB0689 BB0758 BB0806 BB0823 BB0832 BB0844
BBA03 S2 BBA04 S1 BBA05 BBA07 BBA14 OspA BBA15 OspB BBA16 DbpA BBA24 BBA32 BBA33 OppA5 BBA34 BBA36 BBA57
BBA59 Lp6.6 BBA62 P35 BBA64 BBA65 CspA BBA68 BBA69 BBA72 BBB08 BBB09 OppA4 BBB16 OspC BBB19 BBB25 BBB27
RevB BBC10 BBD10 BBE04 BBE08 P35 BBE31 ErpD/Arp BBF01 BBF20 BBG01 BBG25 BBH01 CspZ BBH06 BBH18 BBH32
BBH37 BBI14 BBI16 BBI28 BBI29 P35 BBI36 BBI38 BBI39 BBI42 BBJ01 OspD BBJ09 BBJ34 BBJ36
P35 BBJ41 BBJ47 BBK01 BBK07 BBK12 BBK19 Fbp BBK32 P37 BBK48 P37 BBK50 P23 BBK52 BBK53 MlpH BBL28 ErpN BBL39
ErpO BBL40 RevA1 BBM27 MlpF BBM28 ErpK BBM38 MlpI BBN28 ErpP BBN38 ErpQ BBN39 MlpG BBO28 ErpL BBO39 ErpM BBO40 RevA2 BBP27 MlpA BBP28 ErpA BBP38
ErpB BBP39 BBQ03 P35 BBQ05 MlpJ BBQ35 BBQ46 ErpX BBQ47 BBQ89 MlpD BBR28 ErpH BBR40 ErpY/OspF BBR42 MlpC BBS30 OspG/ErpG BBS41
pK
HisTag
OspA
FlaB
nd
see ErpA BBP38
see ErpB BBP39
see RevA2 BBP27
see BBH01

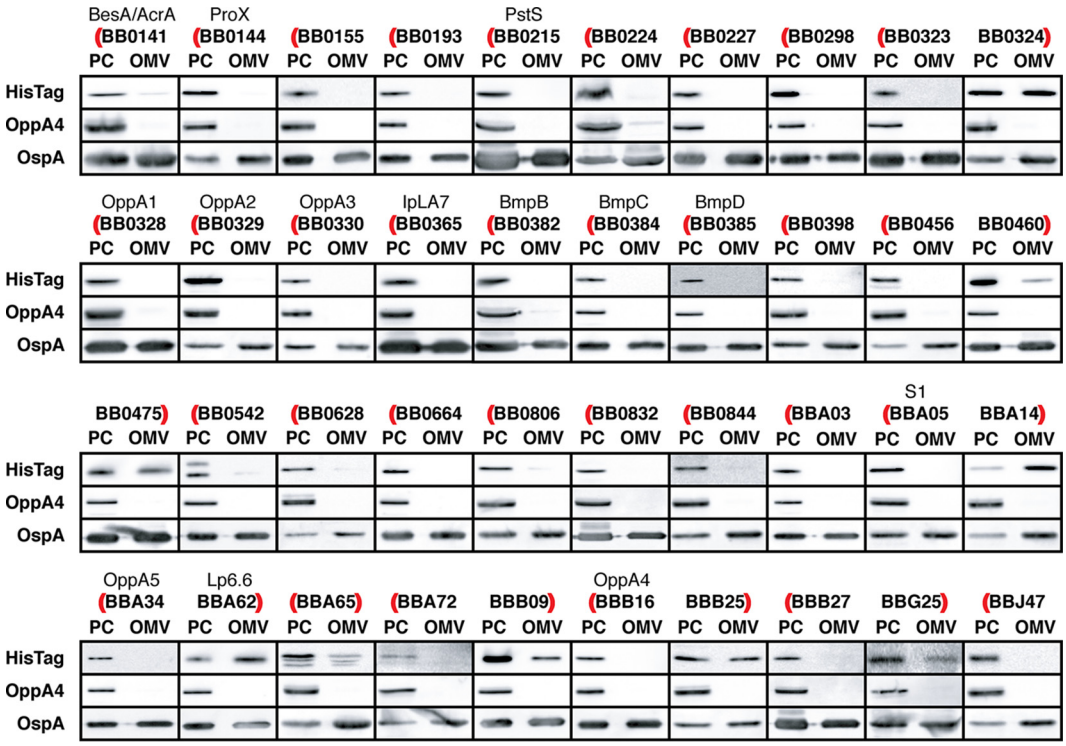

FIG 2 Membrane fractionation of *B. burgdorferi* strains expressing a His-tagged lipoprotein library. Strains that were found to express proteinase K-resistant recombinant lipoproteins were subjected to membrane fractionation using a hypotonic acidic citrate buffer and sucrose gradient to obtain OMVs. Lipoproteins were then localized based on presence or absence in the OMV fraction relative to control proteins. OMVs and PCs were separated by SDS-PAGE, transferred to nitrocellulose, and analyzed by Western blotting using anti-OspA mouse MAb, anti-OppAIV rabbit polyclonal antiserum, or HisProbe-HRP reagent. Lipoproteins are organized by open reading frame with the common name listed, if applicable. Note that the PC fraction is the equivalent of a whole-cell protein preparation partially depleted of OM proteins (see the text). Parentheses flanking the ORF designation indicate the determined lipoprotein localization as follows: (ORF, inner membrane; ORF), outer membrane. The localization of BBA65 remains undetermined due to multiple isoforms with variable distributions. Determined molecular masses of the His-tagged proteins are indicated in Table 1.

mixture of nonspecific proteases that has been shown to digest *B. burgdorferi* proteins that are otherwise protease resistant (84, 107). ErpX was used as a control.

As shown in Fig. 3A, pronase treatment led to complete degradation of OspA, while FlaB remained intact, indicating that assay conditions lead to selective removal of surface-exposed proteins. Parallel treatment of *B. burgdorferi* B31-A3 cells and staining of SDS-PAGE-separated protein samples by Coomassie (Fig. 3B) indicated almost indistinguishable overall proteolysis patterns between proteinase K (pK) and pronase; the only appreciable difference in the pronase-treated sample was the absence of a 51-kDa band that has been attributed to a proteinase K-resistant fragment of the OM porin P66 (108). As expected, the control protein BBQ47 (ErpX) was largely susceptible to degradation by pronase. Three additional lipoproteins, BBA14, BBA65, and BBB25, showed selective degradation by pronase as well. The remaining 6 lipoproteins were found to be pronase resistant in the context of intact cells (Fig. 3A) but readily digested and undetectable when the cells were permeabilized (not shown). This indicated that these 6 proteins are not intrinsically protease resistant but indeed localize to the periplasmic leaflet of the OM. In summary, this set of experiments localized BBA14 and BBB25 to the

FIG 1 Surface proteolysis of *B. burgdorferi* strains expressing a His-tagged lipoprotein library using proteinase K. Intact cells expressing the His-tagged lipoprotein were treated with proteinase K or mock treated as described in the text. Cell lysates were then separated by SDS-PAGE, transferred to nitrocellulose, and analyzed by Western blotting using anti-OspA or anti-FlaB mouse monoclonal antibodies (MAbs) or HisProbe-HRP reagent. Lipoproteins are organized according to open reading frame (ORF) nomenclature (100, 101), with the common name of the protein listed if applicable (Table 1). pK−, untreated mock control; pK+, proteinase K-treated sample. Parentheses flanking the ORF designation indicate the determined lipoprotein localization as follows:))ORF, surface; (ORF), periplasmic. A dot indicates proteins where the consensus localization was ultimately changed to the periplasm [●))ORF] or surface [(ORF)●] due to independent data or follow-up pronase digestion (Fig. 3A). Determined molecular masses of the His-tagged proteins are indicated in Table 1.

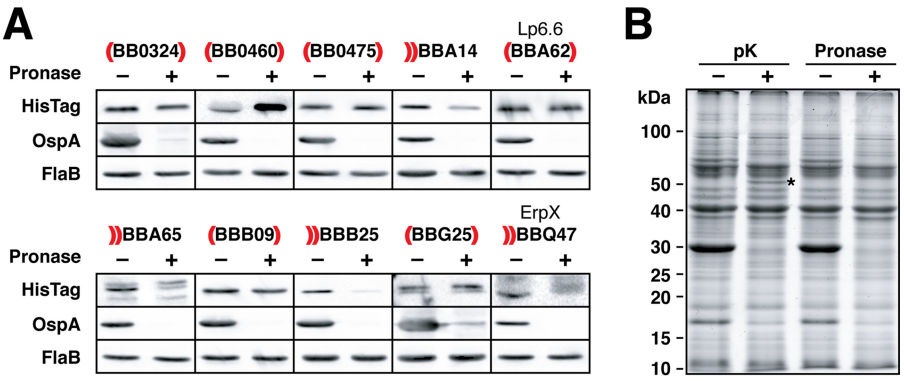

FIG 3 Surface proteolysis of *B. burgdorferi* strains expressing a His-tagged lipoprotein library using pronase. (A) Intact cells expressing His-tagged lipoproteins that were determined to be proteinase K resistant but enriched in the OM were subjected to surface proteolysis with pronase. Cell lysates were then separated by SDS-PAGE and analyzed by Western blotting, as described in the legend to Fig. 1. Pronase −, untreated mock control; pronase +, pronase-treated sample. Parentheses flanking the ORF designation indicate the determined lipoprotein localization as in Fig. 1:))ORF, surface; (ORF), periplasmic. (B) Coomassie-stained SDS-PAGE gel of *B. burgdorferi* strain B31-A3 whole-cell protein preparations obtained before (−) or after (+) incubation with proteinase K or pronase. Protein molecular masses, indicated to the left, were derived from a protein molecular weight marker (Bio-Rad). An asterisk indicates a known proteinase K-resistant, but apparently pronase-sensitive, fragment of integral OM protein P66 (108).

surface *de novo*. BBA65 had been localized previously (74). In that study, the authors found that BBA65 was susceptible to both pronase and proteinase K; the susceptibility to proteinase K could be due to the higher concentration of proteinase K used (400 μg/ml). It also established BB0460, BB0475, BBB09, and BBG25 as additional bona fide P-OM lipoproteins and confirmed the previous localization results for both BB0324 and Lp6.6 (56, 73).

Localization of endogenously expressed lipoproteins by quantitative mass spectrometry. To validate our lipoproteome expression library data with the localization of lipoproteins endogenously expressed by *B. burgdorferi*, we employed quantitative multidimensional protein identification technology (MudPIT) mass spectrometry to analyze the lipoproteome of *B. burgdorferi* B31-A3 (109, 110). Our stock of B31-A3 was shown by multiplex PCR (111) to contain all linear and circular plasmids except for lp5, which is not predicted to encode any lipoproteins (54) (data not shown). Cells were cultured and treated with proteinase K, as described above. To reduce the complexity of the samples, the mock control and proteinase K-treated samples were enriched for membrane-associated proteins by extraction with Triton X-114, as described previously (107). Peptide abundance, expressed as the distributed normalized spectral abundance factor (dNSAF) (112), was captured from two biological replicates and averaged. A comparison of the MudPIT results with the results from our His-tagged lipoprotein assays can be seen in Table 1 and Fig. 4. Eighty-six of the predicted 127 lipoproteins were detectable in *B. burgdorferi* B31-A3 after growth at 34°C in Barbour-Stoenner-Kelly II (BSK-II) culture medium. Among them were 2 of the 3 lipoproteins that were not detectable as His-tagged proteins, BB0536 and BB652 (SecD). The remaining 40 lipoproteins are most likely expressed below the levels detectable by MudPIT under the culture conditions used.

The relative abundance of proteins before and after proteolytic shaving, expressed as a ratio of dNSAF values in the mock control versus the treated samples ($dNSAF_{-pK}$/$dNSAF_{+pK}$), was calculated, ranging from 0.00 (BB0628) to 185.84 (BBA16/OspB). Eleven lipoproteins were undetectable after proteolysis, resulting in an infinite (∞) ratio; for analysis purposes, the values of these proteins were capped at the highest calculated value (185.84). Plotting the dNSAF ratios for the surface and periplasmic lipoprotein cohorts identified in the expression library showed a clear separation (Fig. 4). The mean dNSAF ratio for periplasmic lipoproteins was 0.80 (range, 0.00 to 2.22), which is below but close to the expected ratio of 1.0. One explanation is that surface proteolysis yields a significantly less complex protein sample (Fig. 3B), which may

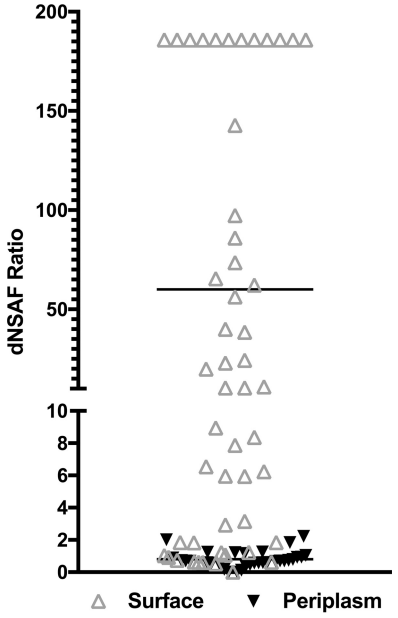

FIG 4 Scatter plot of MudPIT-derived dNSAF ratios of surface and periplasmic lipoproteins. Ratios of dNSAF before treatment with pK to that after proteinase K treatment ($dNSAF_{-pK}/dNSAF_{+pK}$) were calculated for 87 lipoproteins detected by MudPIT and plotted using GraphPad Prism. Horizontal lines indicate the mean dNSAF ratios for surface and subsurface proteins. Note that (i) infinite dNSAF values due to undetectable protein after pK treatment were capped at the highest calculated value of 185.84 for BBA16/OspB and that (ii) surface-assigned proteins that are partially resistant to pK (Fig. 1; see also the text) cluster with subsurface proteins (specific dNSAF values are given in Table 1).

lead to the "unmasking" of previously undetectable/unassignable peptides. Consequently, the ratio's numerator may be depressed relative to the denominator. The mean dNSAF ratio for surface proteins was 60.00 (range, 0.00 to 185.84 [capped {see above}]). Twelve surface-assigned lipoproteins had low dNSAF ratios around or below 1.0. Most of the proteins in this cohort were members of the paralogous Mlp, Rev, and Erp protein families that had shown at least partial resistance to proteinase K in our experiments (Fig. 1) or prior studies (Table 1). Also, 4 of these proteins were subsequently shown to be accessible to *in situ* pronase digestion (Fig. 3A). As shown in Fig. 4, a dNSAF ratio of 2 or above is a high-confidence predictor for surface exposure. This cutoff was statistically confirmed by a Mann-Whitney nonparametric U test using the OriginPro 9.1 software suite. Parallel analysis of sequence coverage, i.e., the percentage of protein sequence covered by detected peptides, before and after pK treatment also showed that a reduction of 10% or higher was a statistically valid predictor of surface exposure (see Fig. S1 and Table S2 in the supplemental material).

Reconciliation of independent localization data produces a consensus localization catalog for the *B. burgdorferi* lipoproteome. Our lipoproteome expression library contained 49 lipoproteins that had been independently localized prior to this study (Table 1). The main rationale for their inclusion in the present study was to use them as internal validation controls. For 41 lipoproteins, the current localization data were in unequivocal agreement with published data. Three lipoproteins, BB0298, BBA05/S1 antigen, and BBA34/OppA5, were more precisely localized within the periplasmic compartment to the IM. Discrepancies with previously published localization data were found for 8 lipoproteins, but all disagreements could be reconciled: (i) a first set of 4 proteins was previously described as surface exposed but was found to be restricted to the periplasm in our assays (Table 1). BmpB (BB0382), like the other homologs of this protein family, was localized by us to the IM. An earlier study had detected BmpB on the surface by immunofluorescence, albeit without controlling for accidental permeabilization of the fragile spirochetal OM (63). OppA1 and OppA2 were also localized to the IM, as were the other homologs of that oligopeptide-

binding lipoprotein family. Again, prior studies had solely relied on immunofluorescence data without controlling for the integrity of the bacterial envelope (60, 61). The fourth protein in this set, BBA03, was also found solely in the IM in the present study. A prior well-controlled localization study remained equivocal in that BBA03 was found by immunofluorescence to be partially surface exposed but at the same time was protected from proteinase K in intact, but not permeabilized, cells (64). (ii) Two IM lipoproteins, BB0227 and BBB27, were localized to the inner leaflet of the OM in one of our earlier studies (57); we now believe that these localization results were erroneous due to contamination of the OMV fraction and a less-stringent interpretation of the data. (iii) BB0323 was localized by us to the IM but was identified by others as an OM periplasmic lipoprotein (59). BB0323 was shown to undergo multistep proteolytic processing in the periplasm (113). Consequently, upon protein maturation, any C-terminal epitope tag will partition together with a C-terminal soluble fragment. Accordingly, we detected only a 14-kDa fragment of the 44-kDa full-length protein in the PC fraction (Table 1). We therefore defer to the previous work on BB0323 as a more accurate reflection of this lipoprotein's localization. (iv) Our final, but probably most intriguing, disagreement with a previous finding was concerning BB0028. This lipoprotein was found to be at least partially surface exposed in our work but has been previously described as a periplasmic OM associated with the OM beta-barrel assembly machinery (BAM) complex (56). In other bacterial systems, BAM lipoprotein modules were shown to assume topologies that expose their C termini on the bacterial surface under certain experimental conditions (51, 114). Thus, we hypothesize that BB0028 transiently and partially (i.e., predominantly via its C terminus) localizes to the surface. Any excess of BB0028 in the *B. burgdorferi* BAM complex may detectably shift the protein's topological equilibrium toward the cell surface.

The aggregation of the present and past data produces a comprehensive and internally validated consensus catalog of lipoprotein localization within the *B. burgdorferi* envelope (Table 1). Of the spirochete's 127 predicted lipoproteins within this set, 125 lipoproteins localize conclusively to either the surface (86), periplasmic leaflet of the OM (8), or the IM (31). The remaining two predicted lipoproteins remained undetectable as epitope-tagged proteins and could not be conclusively localized, but one (BB0536) was detected by mass spectrometry, with a dNSAF ratio consistent with periplasmic localization.

Reassessment of potential *B. burgdorferi* lipoprotein sorting motifs within the N-terminal tethers. Our earlier studies indicated that lipoprotein tether peptides are structurally similar in that they are intrinsically disordered. Yet, they lack any significant peptide sequence homology beyond the N-terminal cysteine residue. Together with our extensive mutational analyses, this led us to conclude that there are no specific canonical peptide motifs that direct lipoproteins to the different envelope compartments of *B. burgdorferi* (57). With the lipoproteome localization data in hand, we decided to reopen this inquiry. Tether peptide sequences from the cohorts of surface, periplasmic OM, and periplasmic IM lipoproteins were aligned and compared. Again, no compartment-specific peptide motifs emerged from this analysis (Fig. 5). A recent study of lipoprotein secretion in the Gram-negative pathogen *Capnocytophaga canimorsus* showed that N-terminal patches of negatively charged Asp and Glu residues in the proper sequential and positional N-terminal context can drive lipoprotein surface localization, and that this surface lipoprotein secretion signal is conserved and recognized in other members of the phylum *Bacteroidetes* (45). While we cannot fully exclude a similar charge-based sorting mechanism in *Borrelia*, barring additional experimentation, we did not detect any positional conservation of negative charges in the 86 *B. burgdorferi* surface lipoproteins (Fig. 5).

DISCUSSION

The lipoprotein repertoire of *B. burgdorferi* is exceptionally large, especially when taking into account the spirochete's small and fragmented genome. Compared to *E. coli*'s 4-Mb circular genome with about 90 lipoprotein genes (46, 47), *B. burgdorferi*'s

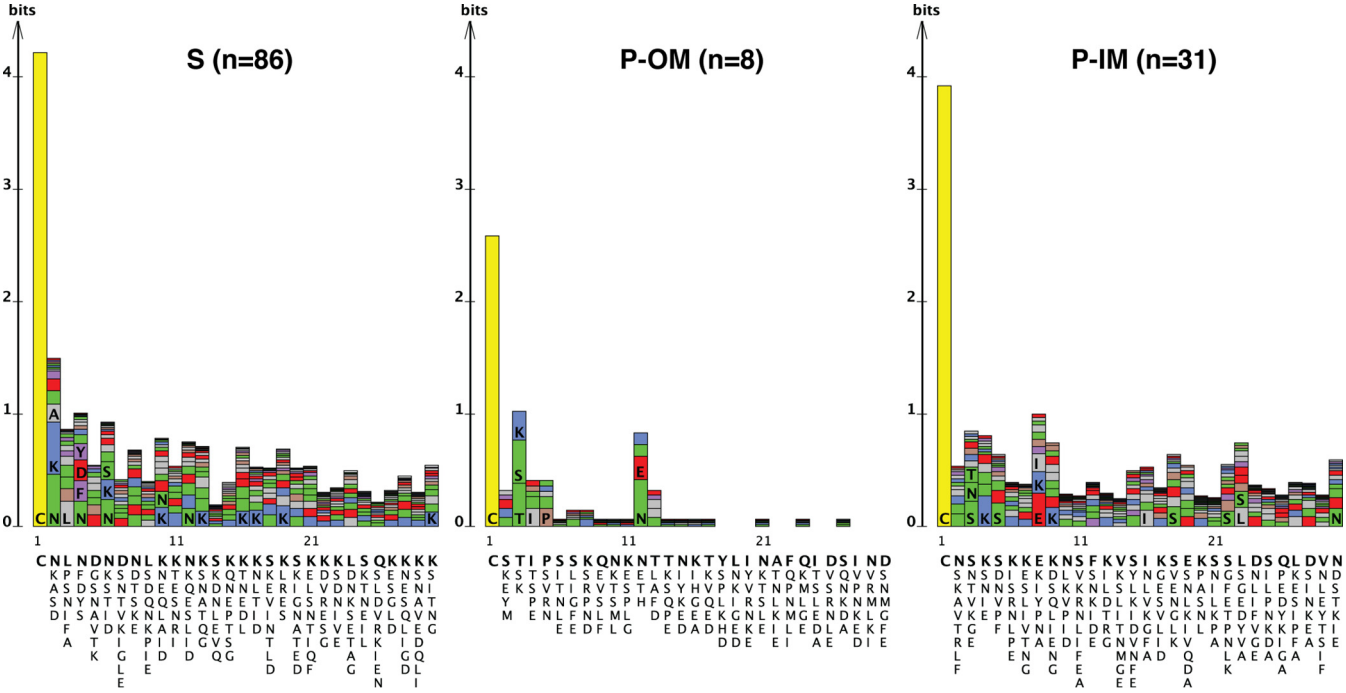

FIG 5 Sequence alignment of *B. burgdorferi* surface, periplasmic OM, or IM lipoprotein tether peptides. A LogoBar (153) representation of the N-terminal sequence of known or predicted mature *B. burgdorferi* lipoproteins (54) illustrates the maintained complexity of surface (S), periplasmic OM (P-OM), and periplasmic IM (P-IM) lipoprotein tether peptides. The height of each column, measured in bits, is proportional to the lack of complexity at a given position. The columns are stacked from the bottom starting with the most frequently occurring residue at that position and continuing upward. Below each column are the six most frequently occurring residues at each position, in order of frequency from top to bottom. Colors indicate residues with similar characteristics (e.g., red for negatively charged Asp and Glu residues).

1.6-Mb genome spread across a linear chromosome, and a collection of linear and circular plasmids encodes over 120 lipoproteins. Since the initial identification of OspA and OspB as common surface antigens of Lyme disease spirochetes (67, 115) 3 decades ago, numerous studies have shown that lipoproteins play an outsized and multifunctional role as virulence factors in the transmission, colonization, dissemination, and persistence of *Borrelia burgdorferi* and the resulting pathology of Lyme disease. Following the precedent of OspA and OspB, much of the research focus has been on identifying additional surface lipoproteins that contribute to *B. burgdorferi*'s interface with the tick vector or host and could serve as vaccine targets. Thus, it may be not surprising that 36 of the 47 additional lipoproteins that were subsequently studied localized to the surface. Together, these studies yielded a rather limited and potentially biased data set, covering less than 40% of the predicted *B. burgdorferi* lipoproteome. In the present study, we have closed this gap in our understanding of the complex cell envelope of *B. burgdorferi* by providing spatial information on 98% of its predicted lipoproteome.

Correlation of gene and protein localization. It has been noted earlier that *B. burgdorferi*'s megabase linear chromosome, and to some degree the cp26 minichromosome, tend to contain essential genes, while the remainder of the circular and linear plasmids appear to be nonessential for growth in culture (101, 116–119). While this generalization at least partially extends to the lipoproteins encoded by these replicons, there is a remarkable correlation of gene localization and protein localization: 79 of the 90 plasmid-encoded lipoproteins (88%) are surface exposed, while only 7 out of the 37 chromosomally encoded lipoproteins (19%) are found on the surface (Table 1). This dichotomy is understandable when considering the biological function and primary protein sequence. Many of the plasmid-encoded lipoproteins share significant homology, which has led to their organization into "paralogous gene families" (101). Instructive examples are the Erp, Mlp, and Pfam54 lipoproteins encoded on the multiple

prophage-related *B. burgdorferi* cp32/lp56 plasmids (101, 120–122). Overall, 62 of the 86 surface lipoproteins (72%) belong to a paralogous group. In contrast, only 14 of the 39 periplasmic lipoproteins (36%) have other paralogs (101) (Table 1). This well-titrated variability and redundancy in surface lipoproteins may stem from the need of *B. burgdorferi* to adapt to a multitude of environments during its enzootic cycle. Chromosomally encoded but surface-localized BB0352 and BB0689 were identified to possess putative sugar- and lipid-binding domains by the HHpred algorithm (123). This suggests that surface lipoproteins encoded by essential genetic elements play housekeeping or metabolic roles. Similarly, subsurface lipoproteins located on nonessential plasmids seem to have a role in transmission and virulence. BBJ47, which we localized to the IM, was identified by HHpred to belong to Pfam17044. This groups BBJ47 with the *B. burgdorferi* BptA proteins and suggests a role in tick persistence (124).

Correlation of lipoprotein localization to *in vivo* expression and immunogenicity. To gain further insight into the biological significance of our data, we explored potential correlations of lipoprotein spatial compartmentalization with temporal expression and immunogenicity (Table 1). Our working lipoproteome data were first cross-referenced with a previous study that examined the reactivity of Lyme borreliosis patient versus control sera to various *B. burgdorferi* proteins (125). Forty-three of the 127 lipoproteins were found in that study to be immunogenic (Table 1). Next, we referenced our data set against a study that looked at the transcription of *B. burgdorferi* genes at various stages of the spirochete's enzootic cycle, using an RNA-hybridized microarray assay that was validated through reverse transcription-quantitative PCR (qRT-PCR) (126). Fifty-three lipoproteins, mostly plasmid encoded and surface localized, were found to have varied roles in the infectious cycle based on significantly different levels of transcripts during tick acquisition, tick persistence, vertebrate transmission, and vertebrate persistence (Table 1). Of note, this data mining approach neglects any proteins that may be essential to the cell but are not differentially regulated between environments. Immunogenic surface lipoproteins expressed during tick acquisition, tick persistence, or vertebrate transmission may work in a preventive setting, similarly to the FDA-approved but no-longer-available OspA vaccine (127). Within this group are BBA04 (S2 antigen), BBA07, BBA16 (OspB), BBB19 (OspC), BBK53, and BBL40 (ErpO). Both OspB and OspC have previously been shown to elicit protection when used to immunize laboratory mice (128, 129). Of the remaining four lipoproteins (BBA04, BBA07, BBK53, and BBL40), BBA07 has been implicated in transmission from the tick to vertebrate host, and BBL40 is part of the Erp protein family, a group of lipoproteins implicated in factor H binding and complement resistance (66, 130).

Mechanistic insights into tether peptide-mediated lipoprotein sorting in diderm bacteria. Our results show that two-thirds of the lipoproteins expressed by *B. burgdorferi* are exported to the cell surface, while the remaining periplasmic lipoproteins are mostly retained in the inner membrane. Whereas the periplasmic OM lipoprotein Lp6.6 is among the most abundant envelope proteins (131), the relative simplicity of the *B. burgdorferi* lipoproteome in the inner leaflet of the OM is unexpected. In *E. coli*, an organism with a diderm membrane architecture similar to that of *B. burgdorferi*, most of the lipoproteins are exported to the OM as well (132), but the majority are not surface exposed (133). A generalization that lipoprotein surface exposure is rare and limited appears to hold for most diderm bacteria, with the emerging exception of the Gram-negative *Bacteroidetes*, such as *Bacteroides fragilis* and *C. capnocytophaga* (43, 45). Yet, the identified charge-based *C. capnocytophaga* lipoprotein secretion signals appear to be restricted to that phylum (45), and the *B. burgdorferi* surface localization determinants identified in our own studies appear to extend only to other members of that expanding genus (99). This hints at significant mechanistic differences in lipoprotein secretion between Gram-negative bacteria and spirochetes. Our current data remain compatible with a lipoprotein secretion model that includes two separate secretion checkpoints: the first checkpoint is set up in the inner membrane (IM), where some lipoproteins are retained and others are released to the OM after completion of N-terminal processing. Whether lipoprotein retention and release are generally mediated by the partial *B. burgdorferi* Lol

pathway (1) and dependent on specific N-terminal tether peptide residues is under investigation. Alternatively, release from the IM may be hindered by functional interactions of folded IM lipoproteins with other IM protein complexes. Multiple lines of evidence point to a similar exclusion mechanism at the second checkpoint in the OM, where periplasmic lipoproteins are blocked from "flipping" through the OM due to assumption of their final tertiary structure (57, 76, 92–94). The *B. burgdorferi* BAM protein BamA was shown to be at least indirectly involved in this process (134), and it remains to be determined if/how the other identified *B. burgdorferi* BAM complex proteins (56, 114), including the IM protein TamB (135), play a role in lipoprotein secretion. Recent work has shown that some *Neisseria* surface lipoproteins are secreted to the surface through the lumen of beta-barrel integral OM proteins (44), but homologs are missing from *Borrelia* genomes. Together, this supports our earlier notions that lipoprotein secretion pathways in *Borrelia* spirochetes are unique.

Conclusions. We have comprehensively localized the *B. burgdorferi* lipoproteome using an epitope-tagged expression library and validated our findings by proteomics and by reconciling our data with prior independent protein localization data. The approaches used, such as the initial reliance on C-terminal epitope tags for protein detection, are not without limitations that will be eliminated only with the generation of protein-specific antibodies and further in-depth studies of the newly localized proteins. Yet, we are confident that the consensus *B. burgdorferi* lipoproteome localization catalog presented here reflects the proteins' native partition in the spirochetal cell envelope. Lyme borreliosis remains the most common vector-borne illness in the United States and is common throughout temperate climates in the Northern Hemisphere, and there are continuing efforts to improve diagnostics and preventive measures. Placing our lipoproteome localization data into the context of genome- and proteome-wide studies may facilitate the identification of additional diagnostic targets and vaccine candidates. The proteomic localization data presented here also provide a predictive framework for proteomic studies of host-pathogen interfaces and envelope structures of other members of the ever-expanding *Borrelia* genus, including the relapsing fever spirochete *Borrelia miyamotoi* (136, 137) and the recently described North American Lyme disease spirochete *Borrelia mayonii* (138, 139).

MATERIALS AND METHODS

Bacterial strains and culture conditions. *E. coli* strains TOP10 and DH5α (Invitrogen) were used for plasmid cloning and propagation. *E. coli* was grown in LB-Miller broth or on LB-Miller agar plates (BD Difco) at 37°C, supplemented with 50 μg/ml kanamycin (Sigma-Aldrich) as necessary. *B. burgdorferi* strain B31-e2, a high-passage-number noninfectious clone of the type strain B31 (140) (provided by Brian Stevenson, University of Kentucky, Lexington, KY), was chosen due to its amenability to transformation and established use in lipoprotein localization assays (57, 76, 94). Additionally, low-passage-number infectious *B. burgdorferi* B31-A3 (109) (provided by Patti Rosa, NIH/NIAID Rocky Mountain Laboratories, Hamilton, MT) was used for proteomic analysis of cellular protein fractions by multidimensional protein identification technology (MudPIT) mass spectrometry. B31-A3 was confirmed to contain all linear and circular plasmids characteristic of strain B31, with the exception of lp5, using a set of multiplex-PCR-compatible oligonucleotide primers (111) (data not shown). *B. burgdorferi* B31-e2 and B31-A3 were maintained in BSK-II complete medium at 34°C containing 300 μg/ml kanamycin, as necessary (141, 142). Recovery of *B. burgdorferi* transformants was performed using semisolid BSK-II medium as described previously (142), with plates incubated at 34°C in a humidified 5% CO_2 atmosphere until the development of colonies.

Construction of an epitope-tagged *B. burgdorferi* lipoprotein expression library. A total of 127 *B. burgdorferi* type strain B31 lipoproteins were selected for the study based on the cumulative list of probable, possible, and false-negative lipoprotein genes identified by the SpLip algorithm (54) (Table 1); of note, this algorithm-based list omits some lipoproteins, such as the variable surface lipoprotein VlsE (143). Genomic DNA from cultured low-passage-number infectious *B. burgdorferi* B31-A3 was isolated (Promega Wizard genomic DNA [gDNA] kit), and lipoprotein genes were amplified by PCR using Phusion HF enzyme (New England BioLabs) with gene-specific oligonucleotide primers (Integrated DNA Technologies) containing 5′ NdeI and XmaI restriction site extensions, respectively (see Table S1 in the supplemental material). The resulting PCR amplicons were digested with NdeI and XmaI and ligated into pSC:LP (Fig. 6), a vector backbone derived from recombinant plasmid pSC1000 (57) by digestion with NdeI and XmaI. pSC1000, a derivative of the *B. burgdorferi-E. coli* shuttle vector pBSV2 (144), expresses the lipoprotein OspA (BBA15) under the constitutive flagellin promoter (P_{flaB}) with a C-terminal His tag; the NdeI (CA′TATG) and XmaI (C′CCGGG) sites are within the start codon and the His tag linker, respectively. Due to *Borrelia* DNA being about 70% AT, this approach allowed for the direct amplification by PCR and

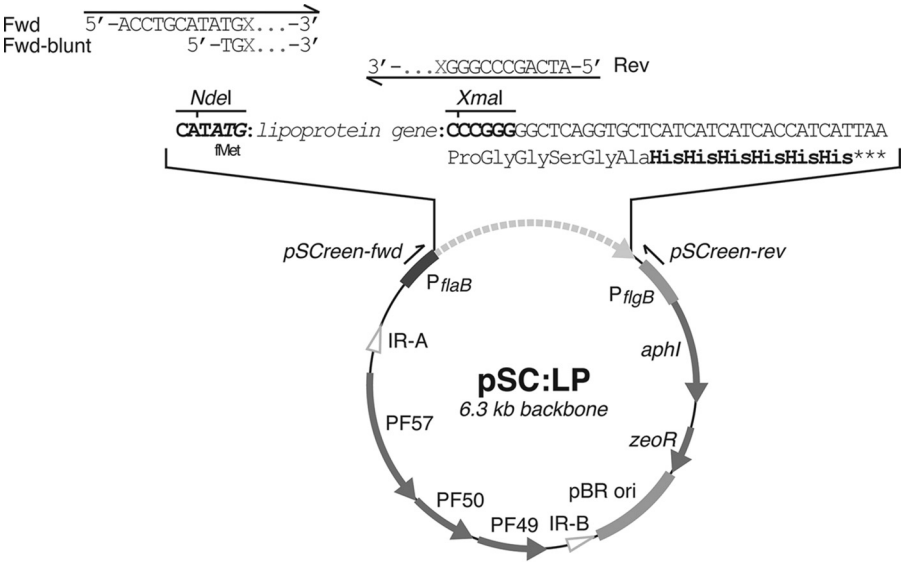

FIG 6 Plasmid map of the *B. burgdorferi* lipoprotein expression library vector backbone pSC-LP. pSC-LP is a derivative of the *B. burgdorferi-E. coli* shuttle vector pBSV2 (57, 144) that drives expression of cloned genes using the *B. burgdorferi flaB* promoter (P_{flaB}) and provides a C-terminal hexahistidine tag preceded by a flexible 6-amino-acid linker peptide. Restriction enzyme sites and primer sequences used for amplification and cloning of lipoprotein genes are indicated (see also Table S1 and the text).

in-frame cloning of 115 *Borrelia* lipoprotein genes. Ten lipoprotein genes containing internal NdeI sequences were amplified and cloned using a modified forward PCR primer that produced an amplicon with a 5′ blunt end compatible with the pSC:LP NdeI site filled in using Klenow (Fig. 6). BB0352 and BBB16 (*oppA4*) were cloned under their native promoters, taken to be within about 150 bp upstream of their respective start codons. Recombinant plasmids were recovered from cultured *E. coli* transformants using the QIAprep spin kit, according to the manufacturer's instructions (Qiagen), and screened for the expected insert by PCR using *Taq* polymerase and a primer pair complementary to pSC:LP sequences 5′ of the NdeI site and 3′ of the XmaI site, respectively (pSCreen-fwd, 5′-AAGGATTTGCCAAAGTCAG-3′; pSCreen-rev, 5′-GTAAAACGACGGCCAG-3′) (Fig. 6 and Table S1). PCR-positive clones were sequenced to verify the expected insert sequence (ACGT; Eton Bioscience). *E. coli* clones harboring the verified recombinant plasmids were stored in LB containing 15% (vol/vol) glycerol at −80°C.

Next, *B. burgdorferi* B31-e2 was transformed with the verified plasmids by electroporation (145), cloned by plating in semisolid BSK-II medium, and expanded in liquid BSK-II medium as described previously (76). Cultures of putative transformants were screened by both PCR using gene-specific primers (see Table S1) and by Western blotting of whole-cell lysates with the HisProbe-HRP reagent (Thermo Fisher), according to the manufacturer's instructions. Clones that expressed epitope-tagged protein were then expanded in BSK-II medium and used in subsequent assays. Verified *B. burgdorferi* clones were stored in BSK-II medium containing 10% (vol/vol) dimethyl sulfoxide (DMSO) at −80°C (142).

Surface proteolysis of intact *B. burgdorferi* spirochetes. Proteolytic shaving of intact spirochetes with proteinase K was performed as described previously (57, 76, 94, 146), with minor modifications. Treatment of cells with pronase (Roche) was performed in accordance with previously published protocols (84, 107) but used the manufacturer's currently recommended reaction conditions (catalog no. 10165921001, version 07; Roche). Briefly, cells were grown at 34°C to late-logarithmic phase in BSK-II medium and harvested by centrifugation at room temperature using a centrifugal force not exceeding 3,000 × *g* using a Sorvall Legend RT centrifuge. Cells were then washed once by resuspension in sterile room-temperature Dulbecco's phosphate-buffered saline (dPBS) containing 5 mM $MgCl_2$ (dPBS + Mg) and repelleted. Cells were then resuspended in dPBS + Mg with either distilled water (dH_2O) (mock), proteinase K (Invitrogen, 200 μg/ml final concentration), or pronase (1 mg/ml final concentration; Roche Life Sciences). Proteinase K-containing samples and respective controls were incubated for 1 h at room temperature, and reactions were stopped after 1 h by adding phenylmethylsulfonyl fluoride (PMSF) to a final concentration of 5 mM (147, 148). Pronase-containing samples and respective controls were incubated for 2 h at 37°C, and reactions were stopped by addition of EDTA, PMSF, and Pefabloc SC to 1 mM, 0.2 mM, and 0.8 mM final concentrations, respectively. Subsequently, cells were pelleted by microcentrifugation, resuspended in SDS-PAGE sample buffer containing 50 mM dithiothreitol (DTT; final concentration), boiled for 5 min, and stored at −20°C until analysis by SDS-PAGE (149).

Isolation of *B. burgdorferi* OMVs. OMVs from spirochetes were isolated as previously described (57, 76, 94, 106). Briefly, cells were grown to early exponential phase, harvested, and washed with dPBS containing 0.1% (wt/vol) bovine serum albumin. Cells were then resuspended in 25 mM sodium citrate (pH 3.2) containing 0.1% (wt/vol) bovine serum albumin (BSA) (citrate buffer + BSA). Cell suspensions were shaken for 2 h at room temperature in a New Brunswick C24 incubator at 250 rpm to release OMVs, at which point the cell suspension was harvested, resuspended in citrate buffer + BSA, and loaded onto

a discontinuous 56/42/25% (wt/wt) sucrose gradient in citrate buffer without BSA. Cell suspensions were centrifuged at 100,000 × *g* for 18 h at 4°C in a Beckman Coulter XPN-80 ultracentrifuge using a SW 32 Ti rotor and Beckman UltraClear tubes, and the resulting upper (OMV) bands and lower (protoplasmic cylinder [PC]) bands were separated by needle aspiration. Fractions were diluted in cold dPBS, repelleted separately, and then resuspended in dPBS containing 1 mM PMSF. A portion of the resuspended fractions was used to prepare SDS-PAGE samples and stored at −20°C after boiling. The remainder of the sample was stored at −80°C for later analysis.

SDS-PAGE analysis and immunoblotting. SDS-PAGE analysis and immunoblotting were performed as described previously (57, 76, 94). Protein samples were prepared as described above and separated using a 12% SDS-polyacrylamide gel (Bio-Rad). After transfer, gels were either Coomassie stained for total protein determination (EZ-Run protein gel staining solution; Fisher) or were transferred to nitrocellulose membranes (Amersham, GE Healthcare) using a Trans-Blot SD apparatus (Bio-Rad). Membranes were then blocked posttransfer with either 5% (wt/vol) nonfat dry milk or 2.5% (wt/vol) BSA and probed with mouse anti-FlaB (1:300 dilution; catalog no. H9724 [150]), mouse anti-OspA (1:1,000 dilution; catalog no. H5332 [67]), rabbit polyclonal anti-OppAIV (1:1,500 dilution [151]), or the HisProbe-HRP reagent, according to the manufacturer's instructions. H9724 and H5332 antibodies were a gift from Alan Barbour (University of California at Irvine, CA), and anti-OppAIV antibody was generously provided by Patricia Rosa (NIH/NIAID Rocky Mountain Laboratories, Hamilton, MT). Blots were treated with corresponding alkaline phosphatase (AP)-conjugated secondary antibodies (1:30,000 dilution; catalog no. A3562 and A3687; Sigma-Aldrich) and developed using LumiPhos (Thermo Fisher, now discontinued) or Immun-Star AP (Bio-Rad). Blots probed with HisProbe-HRP reagent were developed with SuperSignal West Dura reagent (Thermo Fisher). Signals were detected and captured using a Fujifilm LAS-4000 charge-coupled-device (CCD) imager and further processed with Adobe Photoshop CS6.

Analysis of protein fractions by MudPIT. Localization of lipoproteins endogenously expressed under standard culture conditions was determined using multidimensional protein identification technology (MudPIT) mass spectrometry (152). *B. burgdorferi* B31-A3 cells were subjected to surface proteolysis with proteinase K, as described above. Membrane-associated proteins were then enriched by overnight extraction of the mock- and proteinase K-treated samples with Triton X-114, as described previously (107). The washed detergent extracts were then precipitated overnight using acetone (80% [vol/vol]), resuspended in 0.1 M Tris-HCl (pH 8.5), and precipitated again overnight using trichloroacetic acid (TCA; 20% [vol/vol]). The addition of acetone precipitation in the protocol was necessary to effectively remove detergent prior to analysis by MudPIT. Two biological replicates of the resulting desiccated frozen protein samples were then submitted for MudPIT analysis (Proteomics Center, Stowers Institute for Medical Research, Kansas City, MO). Resuspended protein samples were digested with endoproteinases Lys-C (Roche) and trypsin (Promega) at 0.1 μg/μl final concentration each. The protease-digested samples were then analyzed by MudPIT on an LTQ linear ion trap (Thermo Scientific) coupled to a Quaternary Agilent 1100 series high-performance liquid chromatograph (HPLC) (110). Protein content in mock control versus proteinase K-treated whole-cell protein preparations was analyzed by comparison of the average distributed normalized spectral abundance factor (dNSAF) for each unique protein, which correlates directly with the relative abundance of a particular protein in the sample (112). A dNSAF ratio of control to protease-treated sample ($dNSAF_{-pK}/dNSAF_{+pK}$) was calculated for each detected protein. Theoretically, a ratio of 1 indicates that the protein is as abundant after surface proteolysis as before, i.e., not susceptible to proteinase K due to either periplasmic localization or intrinsic resistance to protease. Conversely, a ratio greater than 1 indicates that a protein is less abundant after proteolytic shaving, i.e., is surface exposed.

Accession number(s). All mass spectrometry data are available from the ProteomeXchange repository under accession number PXD005617 (http://proteomecentral.proteomexchange.org/cgi/GetDataset?ID=PXD005617).

SUPPLEMENTAL MATERIAL

Supplemental material for this article may be found at https://doi.org/10.1128/JB.00658-16.

TEXT S1, PDF file, 0.8 MB.

ACKNOWLEDGMENTS

We thank Brian Stevenson, Alan Barbour, and Patti Rosa for supplying bacterial strains and antibodies, Eszter Adany, Ariel Dunn, and Erin Andres for technical support, and Joe Lutkenhaus, Michael Parmely, Indranil Biswas, and Mark Fisher for helpful discussions during the course of the project.

This work was supported in part by NIH grants R01 AI063261 and R21 AI113547 (to W.R.Z.), P30 GM103326 (COBRE pilot grant to W.R.Z.), and P20 RR016475 (K-INBRE summer fellowship to M.D.M.) and the University of Kansas Medical Center Biomedical Research Training Program (BRTP graduate fellowship to A.S.D.). L.F. and S.K.S. are supported by the Stowers Institute for Medical Research.

REFERENCES

1. Zückert WR. 2014. Secretion of bacterial lipoproteins: through the cytoplasmic membrane, the periplasm and beyond. Biochim Biophys Acta 1843:1509–1516. https://doi.org/10.1016/j.bbamcr.2014.04.022.
2. Szewczyk J, Collet JF. 2016. The journey of lipoproteins through the cell: one birthplace, multiple destinations. Adv Microb Physiol 69:1–50. https://doi.org/10.1016/bs.ampbs.2016.07.003.
3. Kovacs-Simon A, Titball R, Michell S. 2011. Lipoproteins of bacterial pathogens. Infect Immun 79:548–561. https://doi.org/10.1128/IAI.00682-10.
4. von Heijne G. 1989. The structure of signal peptides from bacterial lipoproteins. Protein Eng 2:531–534. https://doi.org/10.1093/protein/2.7.531.
5. Sankaran K, Wu H. 1993. Bacterial lipoproteins, p 163–181. *In* Schlesinger M (ed), Lipid modifications of proteins. CRC Press, Boca Raton, FL.
6. Fröderberg L, Houben E, Baars L, Luirink J, de Gier J. 2004. Targeting and translocation of two lipoproteins in *Escherichia coli* via the SRP/Sec/YidC pathway. J Biol Chem 279:31026–31032. https://doi.org/10.1074/jbc.M403229200.
7. Feltcher M, Gibbons H, Ligon L, Braunstein M. 2013. Protein export by the mycobacterial SecA2 system is determined by the preprotein mature domain. J Bacteriol 195:672–681. https://doi.org/10.1128/JB.02032-12.
8. De Buck E, Lebeau I, Maes L, Geukens N, Meyen E, Van Mellaert L, Anne J, Lammertyn E. 2004. A putative twin-arginine translocation pathway in *Legionella pneumophila*. Biochem Biophys Res Commun 317:654–661. https://doi.org/10.1016/j.bbrc.2004.03.091.
9. Dilks K, Gimenez M, Pohlschroder M. 2005. Genetic and biochemical analysis of the twin-arginine translocation pathway in halophilic archaea. J Bacteriol 187:8104–8113. https://doi.org/10.1128/JB.187.23.8104-8113.2005.
10. Giménez M, Dilks K, Pohlschroder M. 2007. *Haloferax volcanii* twin-arginine translocation substates include secreted soluble, C-terminally anchored and lipoproteins. Mol Microbiol 66:1597–1606. https://doi.org/10.1111/j.1365-2958.2007.06034.x.
11. Widdick D, Dilks K, Chandra G, Bottrill A, Naldrett M, Pohlschroder M, Palmer T. 2006. The twin-arginine translocation pathway is a major route of protein export in *Streptomyces coelicolor*. Proc Natl Acad Sci U S A 103:17927–17932. https://doi.org/10.1073/pnas.0607025103.
12. Arambula D, Wong W, Medhekar B, Guo H, Gingery M, Czornyj E, Liu M, Dey S, Ghosh P, Miller J. 2013. Surface display of a massively variable lipoprotein by a *Legionella* diversity-generating retroelement. Proc Natl Acad Sci U S A 110:8212–8217. https://doi.org/10.1073/pnas.1301366110.
13. Sankaran K, Wu HC. 1994. Lipid modification of bacterial prolipoprotein. Transfer of diacylglyceryl moiety from phosphatidylglycerol. J Biol Chem 269:19701–19706.
14. Tokunaga M, Tokunaga H, Wu H. 1982. Post-translational modification and processing of *Escherichia coli* prolipoprotein *in vitro*. Proc Natl Acad Sci U S A 79:2255–2259. https://doi.org/10.1073/pnas.79.7.2255.
15. Jackowski S, Rock CO. 1986. Transfer of fatty acids from the 1-position of phosphatidylethanolamine to the major outer membrane lipoprotein of *Escherichia coli*. J Biol Chem 261:11328–11333.
16. Gupta SD, Dowhan W, Wu HC. 1991. Phosphatidylethanolamine is not essential for the *N*-acylation of apolipoprotein in *Escherichia coli*. J Biol Chem 266:9983–9986.
17. Hillmann F, Argentini M, Buddelmeijer N. 2011. Kinetics and phospholipid specificity of apolipoprotein *N*-acyltransferase. J Biol Chem 286:27936–27946. https://doi.org/10.1074/jbc.M111.243519.
18. Nakayama H, Kurokawa K, Lee BL. 2012. Lipoproteins in bacteria: structures and biosynthetic pathways. FEBS J 279:4247–4268. https://doi.org/10.1111/febs.12041.
19. Vidal-Ingigliardi D, Lewenza S, Buddelmeijer N. 2007. Identification of essential residues in apolipoprotein *N*-acyl transferase, a member of the CN hydrolase family. J Bacteriol 189:4456–4464. https://doi.org/10.1128/JB.00099-07.
20. Tschumi A, Nai C, Auchli Y, Hunziker P, Gehrig P, Keller P, Grau T, Sander P. 2009. Identification of apolipoprotein *N*-acyltransferase (Lnt) in mycobacteria. J Biol Chem 284:27146–27156. https://doi.org/10.1074/jbc.M109.022715.
21. Okuda S, Tokuda H. 2011. Lipoprotein sorting in bacteria. Annu Rev Microbiol 65:239–259. https://doi.org/10.1146/annurev-micro-090110-102859.
22. Matsuyama S, Tajima T, Tokuda H. 1995. A novel periplasmic carrier protein involved in the sorting and transport of *Escherichia coli* lipoproteins destined for the outer membrane. EMBO J 14:3365–3372.
23. Matsuyama S, Yokota N, Tokuda H. 1997. A novel outer membrane lipoprotein, LolB (HemM), involved in the LolA (p20)-dependent localization of lipoproteins to the outer membrane of *Escherichia coli*. EMBO J 16:6947–6955. https://doi.org/10.1093/emboj/16.23.6947.
24. Ito Y, Matsuzawa H, Matsuyama S, Narita S, Tokuda H. 2006. Genetic analysis of the mode of interplay between an ATPase subunit and membrane subunits of the lipoprotein-releasing ATP-binding cassette transporter LolCDE. J Bacteriol 188:2856–2864. https://doi.org/10.1128/JB.188.8.2856-2864.2006.
25. Yakushi T, Masuda K, Narita S, Matsuyama S, Tokuda H. 2000. A new ABC transporter mediating the detachment of lipid-modified proteins from membranes. Nat Cell Biol 2:212–218. https://doi.org/10.1038/35008635.
26. Yakushi T, Yokota N, Matsuyama S, Tokuda H. 1998. LolA-dependent release of a lipid-modified protein from the inner membrane of *Escherichia coli* requires nucleoside triphosphate. J Biol Chem 273:32576–32581. https://doi.org/10.1074/jbc.273.49.32576.
27. D'Enfert C, Pugsley A. 1989. *Klebsiella pneumoniae pulS* gene encodes an outer membrane lipoprotein required for pullulanase secretion. J Bacteriol 171:3673–3679. https://doi.org/10.1128/jb.171.7.3673-3679.1989.
28. Anderson J, Sparling P, Cornelissen C. 1994. Gonococcal transferrin-binding protein 2 facilitates but is not essential for transferrin utilization. J Bacteriol 176:3162–3170. https://doi.org/10.1128/jb.176.11.3162-3170.1994.
29. Ostberg KL, DeRocco AJ, Mistry SD, Dickinson MK, Cornelissen CN. 2013. Conserved regions of gonococcal TbpB are critical for surface exposure and transferrin iron utilization. Infect Immun 81:3442–3450. https://doi.org/10.1128/IAI.00280-13.
30. Pettersson A, Prinz T, Umar A, van der Biezen J, Tommassen J. 1998. Molecular characterization of LbpB, the second lactoferrin-binding protein of *Neisseria meningitidis*. Mol Microbiol 27:599–610. https://doi.org/10.1046/j.1365-2958.1998.00707.x.
31. Leuzzi R, Serino L, Scarselli M, Savino S, Fontana M, Monaci E, Taddei A, Fischer G, Rappuoli R, Pizza M. 2005. Ng-MIP, a surface-exposed lipoprotein of *Neisseria gonorrhoeae*, has a peptidyl-prolyl *cis*/*trans* isomerase (PPIase) activity and is involved in persistence in macrophages. Mol Microbiol 58:669–681. https://doi.org/10.1111/j.1365-2958.2005.04859.x.
32. Dashper SG, Hendtlass A, Slakeski N, Jackson C, Cross KJ, Brownfield L, Hamilton R, Barr I, Reynolds EC. 2000. Characterization of a novel outer membrane hemin-binding protein of *Porphyromonas gingivalis*. J Bacteriol 182:6456–6462. https://doi.org/10.1128/JB.182.22.6456-6462.2000.
33. Pride AC, Herrera CM, Guan Z, Giles DK, Trent MS. 2013. The outer surface lipoprotein VolA mediates utilization of exogenous lipids by *Vibrio cholerae*. mBio 4(3):e00305–13. https://doi.org/10.1128/mBio.00305-13.
34. van Ulsen P, van Alphen L, ten Hove J, Fransen F, van der Ley P, Tommassen J. 2003. A neisserial autotransporter NalP modulating the processing of other autotransporters. Mol Microbiol 50:1017–1030. https://doi.org/10.1046/j.1365-2958.2003.03773.x.
35. Roussel-Jazédé V, Grijpstra J, van Dam V, Tommassen J, van Ulsen P. 2013. Lipidation of the autotransporter NalP of *Neisseria meningitidis* is required for its function in the release of cell-surface-exposed proteins. Microbiology 159:286–295. https://doi.org/10.1099/mic.0.063982-0.
36. Coutte L, Willery E, Antoine R, Drobecq H, Locht C, Jacob-Dubuisson F. 2003. Surface anchoring of bacterial subtilisin important for maturation function. Mol Microbiol 49:529–539. https://doi.org/10.1046/j.1365-2958.2003.03573.x.
37. Jin S, Joe A, Lynett J, Hani E, Sherman P, Chan V. 2001. JlpA, a novel surface-exposed lipoprotein specific to *Campylobacter jejuni*, mediates adherence to host epithelial cells. Mol Microbiol 39:1225–1236. https://doi.org/10.1111/j.1365-2958.2001.02294.x.
38. Manfredi P, Renzi F, Mally M, Sauteur L, Schmaler M, Moes S, Jeno P, Cornelis G. 2011. The genome and surface proteome of *Capnocytophaga canimorsus* reveal a key role of glycan foraging systems in host glycoproteins deglycosylation. Mol Microbiol 81:1050–1060. https://doi.org/10.1111/j.1365-2958.2011.07750.x.
39. Manning P, Beutin L, Achtman M. 1980. Outer membrane of *Escherichia*

coli: properties of the F sex factor traT protein which is involved in surface exclusion. J Bacteriol 142:285–294.
40. Drummelsmith J, Whitfield C. 2000. Translocation of group 1 capsular polysaccharide to the surface of *Escherichia coli* requires a multimeric complex in the outer membrane. EMBO J 19:57–66. https://doi.org/10.1093/emboj/19.1.57.
41. Robinson L, Ashman E, Hultgren S, Chapman M. 2006. Secretion of curli fibre subunits is mediated by the outer membrane-localized CsgG protein. Mol Microbiol 59:870–881. https://doi.org/10.1111/j.1365-2958.2005.04997.x.
42. Cowles C, Li Y, Semmelhack M, Cristea I, Silhavy T. 2011. The free and bound forms of Lpp occupy distinct subcellular locations in *Escherichia coli*. Mol Microbiol 79:1168–1181. https://doi.org/10.1111/j.1365-2958.2011.07539.x.
43. Wilson MM, Anderson DE, Bernstein HD. 2015. Analysis of the outer membrane proteome and secretome of *Bacteroides fragilis* reveals a multiplicity of secretion mechanisms. PLoS One 10:e0117732. https://doi.org/10.1371/journal.pone.0117732.
44. Hooda Y, Lai CC, Judd A, Buckwalter CM, Shin HE, Gray-Owen SD, Moraes TF. 2016. Slam is an outer membrane protein that is required for the surface display of lipidated virulence factors in *Neisseria*. Nat Microbiol 1:16009. https://doi.org/10.1038/nmicrobiol.2016.9.
45. Lauber F, Cornelis GR, Renzi F. 2016. Identification of a new lipoprotein export signal in Gram-negative bacteria. mBio 7(5):e01232–16. https://doi.org/10.1128/mBio.01232-16.
46. Brokx SJ, Ellison M, Locke T, Bottorff D, Frost L, Weiner JH. 2004. Genome-wide analysis of lipoprotein expression in *Escherichia coli* MG1655. J Bacteriol 186:3254–3258. https://doi.org/10.1128/JB.186.10.3254-3258.2004.
47. Tokuda H, Matsuyama S, Tanaka-Masuda K. 2007. Structure, function, and transport of lipoproteins in *Escherichia coli*, p 67–79. *In* Ehrmann M (ed), The periplasm. ASM Press, Washington, DC.
48. Dong C, Beis K, Nesper J, Brunkan-Lamontagne A, Clarke B, Whitfield C, Naismith J. 2006. Wza the translocon for *E. coli* capsular polysaccharides defines a new class of membrane protein. Nature 444:226–229. https://doi.org/10.1038/nature05267.
49. Cho SH, Szewczyk J, Pesavento C, Zietek M, Banzhaf M, Roszczenko P, Asmar A, Laloux G, Hov AK, Leverrier P, Van der Henst C, Vertommen D, Typas A, Collet JF. 2014. Detecting envelope stress by monitoring beta-barrel assembly. Cell 159:1652–1664. https://doi.org/10.1016/j.cell.2014.11.045.
50. Konovalova A, Perlman DH, Cowles CE, Silhavy TJ. 2014. Transmembrane domain of surface-exposed outer membrane lipoprotein RcsF is threaded through the lumen of beta-barrel proteins. Proc Natl Acad Sci U S A 111:E4350–4358. https://doi.org/10.1073/pnas.1417138111.
51. Webb CT, Selkrig J, Perry AJ, Noinaj N, Buchanan S, Lithgow T. 2012. Dynamic association of BAM complex modules includes surface exposure of the lipoprotein BamC. J Mol Biol 422:545–555. https://doi.org/10.1016/j.jmb.2012.05.035.
52. Michel LV, Shaw J, MacPherson V, Barnard D, Bettinger J, D'Arcy B, Surendran N, Hellman J, Pichichero ME. 2015. Dual orientation of the outer membrane lipoprotein Pal in *Escherichia coli*. Microbiology 161:1251–1259. https://doi.org/10.1099/mic.0.000084.
53. Bergström S, Zückert W. 2010. Structure, function and biogenesis of the *Borrelia* cell envelope, p 139–166. *In* Samuels D, Radolf J (ed), Borrelia: molecular biology, host interaction and pathogenesis. Caister Academic Press, Norwich, United Kingdom.
54. Setubal JC, Reis M, Matsunaga J, Haake DA. 2006. Lipoprotein computational prediction in spirochaetal genomes. Microbiology 152:113–121. https://doi.org/10.1099/mic.0.28317-0.
55. Radolf J, Caimano M, Stevenson B, Hu L. 2012. Of ticks, mice and men: understanding the dual-host lifestyle of Lyme disease spirochaetes. Nat Rev Microbiol 10:87–99.
56. Lenhart TR, Kenedy MR, Yang X, Pal U, Akins DR. 2012. BB0324 and BB0028 are constituents of the *Borrelia burgdorferi* beta-barrel assembly machine (BAM) complex. BMC Microbiol 12:60. https://doi.org/10.1186/1471-2180-12-60.
57. Schulze R, Chen S, Kumru O, Zückert W. 2010. Translocation of *Borrelia burgdorferi* surface lipoprotein OspA through the outer membrane requires an unfolded conformation and can initiate at the C-terminus. Mol Microbiol 76:1266–1278. https://doi.org/10.1111/j.1365-2958.2010.07172.x.
58. Brooks CS, Vuppala SR, Jett AM, Akins DR. 2006. Identification of *Borrelia burgdorferi* outer surface proteins. Infect Immun 74:296–304. https://doi.org/10.1128/IAI.74.1.296-304.2006.
59. Zhang X, Yang X, Kumar M, Pal U. 2009. BB0323 function is essential for *Borrelia burgdorferi* virulence and persistence through tick-rodent transmission cycle. J Infect Dis 200:1318–1330. https://doi.org/10.1086/605846.
60. Hu LT, Pratt SD, Perides G, Katz L, Rogers RA, Klempner MS. 1997. Isolation, cloning, and expression of a 70-kilodalton plasminogen binding protein of *Borrelia burgdorferi*. Infect Immun 65:4989–4995.
61. Das S, Shraga D, Gannon C, Lam TT, Feng S, Brunet LR, Telford SR, Barthold SW, Flavell RA, Fikrig E. 1996. Characterization of a 30-kDa *Borrelia burgdorferi* substrate-binding protein homologue. Res Microbiol 147:739–751. https://doi.org/10.1016/S0923-2508(97)85121-2.
62. von Lackum K, Ollison K, Bykowski T, Nowalk A, Hughes J, Carroll J, Zückert W, Stevenson B. 2007. Regulated synthesis of the *Borrelia burgdorferi* inner-membrane lipoprotein lpLA7 (P22, P22-A) during the Lyme disease spirochaete's mammal-tick infectious cycle. Microbiology 153:1361–1371. https://doi.org/10.1099/mic.0.2006/003350-0.
63. Pal U, Wang P, Bao F, Yang X, Samanta S, Schoen R, Wormser GP, Schwartz I, Fikrig E. 2008. *Borrelia burgdorferi* basic membrane proteins A and B participate in the genesis of Lyme arthritis. J Exp Med 205:133–141. https://doi.org/10.1084/jem.20070962.
64. Bestor A, Rego RO, Tilly K, Rosa PA. 2012. Competitive advantage of *Borrelia burgdorferi* with outer surface protein BBA03 during tick-mediated infection of the mammalian host. Infect Immun 80:3501–3511. https://doi.org/10.1128/IAI.00521-12.
65. Xu H, He M, Pang X, Xu ZC, Piesman J, Yang XF. 2010. Characterization of the highly regulated antigen BBA05 in the enzootic cycle of *Borrelia burgdorferi*. Infect Immun 78:100–107. https://doi.org/10.1128/IAI.01008-09.
66. Xu H, He M, He JJ, Yang XF. 2010. Role of the surface lipoprotein BBA07 in the enzootic cycle of *Borrelia burgdorferi*. Infect Immun 78:2910–2918. https://doi.org/10.1128/IAI.00372-10.
67. Barbour AG, Tessier SL, Todd WJ. 1983. Lyme disease spirochetes and ixodid tick spirochetes share a common surface antigenic determinant defined by a monoclonal antibody. Infect Immun 41:795–804.
68. Barbour AG, Tessier SL, Hayes SF. 1984. Variation in a major surface protein of Lyme disease spirochetes. Infect Immun 45:94–100.
69. Hanson MS, Cassatt DR, Guo BP, Patel NK, McCarthy MP, Dorward DW, Hook M. 1998. Active and passive immunity against *Borrelia burgdorferi* decorin binding protein A (DbpA) protects against infection. Infect Immun 66:2143–2153.
70. Zhi H, Weening EH, Barbu EM, Hyde JA, Hook M, Skare JT. 2015. The BBA33 lipoprotein binds collagen and impacts *Borrelia burgdorferi* pathogenesis. Mol Microbiol 96:68–83. https://doi.org/10.1111/mmi.12921.
71. Raju BV, Esteve-Gassent MD, Karna SL, Miller CL, Van Laar TA, Seshu J. 2011. Oligopeptide permease A5 modulates vertebrate host-specific adaptation of *Borrelia burgdorferi*. Infect Immun 79:3407–3420. https://doi.org/10.1128/IAI.05234-11.
72. Yang X, Qin J, Promnares K, Kariu T, Anderson JF, Pal U. 2013. Novel microbial virulence factor triggers murine Lyme arthritis. J Infect Dis 207:907–918. https://doi.org/10.1093/infdis/jis930.
73. Lahdenne P, Porcella SF, Hagman KE, Akins DR, Popova TG, Cox DL, Katona LI, Radolf JD, Norgard MV. 1997. Molecular characterization of a 6.6-kilodalton *Borrelia burgdorferi* outer membrane-associated lipoprotein (lp6.6) which appears to be downregulated during mammalian infection. Infect Immun 65:412–421.
74. Hughes JL, Nolder CL, Nowalk AJ, Clifton DR, Howison RR, Schmit VL, Gilmore RD, Jr, Carroll JA. 2008. *Borrelia burgdorferi* surface-localized proteins expressed during persistent murine infection are conserved among diverse *Borrelia* spp. Infect Immun 76:2498–2511. https://doi.org/10.1128/IAI.01583-07.
75. Kraiczy P, Hellwage J, Skerka C, Becker H, Kirschfink M, Simon MM, Brade V, Zipfel PF, Wallich R. 2004. Complement resistance of *Borrelia burgdorferi* correlates with the expression of BbCRASP-1, a novel linear plasmid-encoded surface protein that interacts with human factor H and FHL-1 and is unrelated to Erp proteins. J Biol Chem 279:2421–2429. https://doi.org/10.1074/jbc.M308343200.
76. Schulze RJ, Zückert WR. 2006. *Borrelia burgdorferi* lipoproteins are secreted to the outer surface by default. Mol Microbiol 59:1473–1484. https://doi.org/10.1111/j.1365-2958.2006.05039.x.
77. Fuchs R, Jauris S, Lottspeich F, Preac-Mursic V, Wilske B, Soutschek E. 1992. Molecular analysis and expression of a *Borrelia burgdorferi* gene encoding a 22 kDa protein (pC) in *Escherichia coli*. Mol Microbiol 6:503–509. https://doi.org/10.1111/j.1365-2958.1992.tb01495.x.
78. Zhang L, Zhang Y, Adusumilli S, Liu L, Narasimhan S, Dai J, Zhao YO,

Fikrig E. 2011. Molecular interactions that enable movement of the Lyme disease agent from the tick gut into the hemolymph. PLoS Pathog 7:e1002079. https://doi.org/10.1371/journal.ppat.1002079.
79. Hartmann K, Corvey C, Skerka C, Kirschfink M, Karas M, Brade V, Miller JC, Stevenson B, Wallich R, Zipfel PF, Kraiczy P. 2006. Functional characterization of BbCRASP-2, a distinct outer membrane protein of *Borrelia burgdorferi* that binds host complement regulators factor H and FHL-1. Mol Microbiol 61:1220–1236. https://doi.org/10.1111/j.1365-2958.2006.05318.x.
80. Labandeira-Rey M, Baker EA, Skare JT. 2001. VraA (BBI16) protein of *Borrelia burgdorferi* is a surface-exposed antigen with a repetitive motif that confers partial protection against experimental Lyme borreliosis. Infect Immun 69:1409–1419. https://doi.org/10.1128/IAI.69.3.1409-1419.2001.
81. Norris SJ, Carter CJ, Howell JK, Barbour AG. 1992. Low-passage-associated proteins of *Borrelia burgdorferi* B31: characterization and molecular cloning of OspD, a surface-exposed, plasmid-encoded lipoprotein. Infect Immun 60:4662–4672.
82. Coleman AS, Pal U. 2009. BBK07, a dominant *in vivo* antigen of *Borrelia burgdorferi*, is a potential marker for serodiagnosis of Lyme disease. Clin Vaccine Immunol 16:1569–1575. https://doi.org/10.1128/CVI.00301-09.
83. Probert WS, Johnson BJ. 1998. Identification of a 47 kDa fibronectin-binding protein expressed by *Borrelia burgdorferi* isolate B31. Mol Microbiol 30:1003–1015. https://doi.org/10.1046/j.1365-2958.1998.01127.x.
84. El-Hage N, Babb K, Carroll JA, Lindstrom N, Fischer ER, Miller JC, Gilmore RD, Jr, Mbow ML, Stevenson B. 2001. Surface exposure and protease insensitivity of *Borrelia burgdorferi* Erp (OspEF-related) lipoproteins. Microbiology 147:821–830. https://doi.org/10.1099/00221287-147-4-821.
85. Carroll JA, El-Hage N, Miller JC, Babb K, Stevenson B. 2001. *Borrelia burgdorferi* RevA antigen is a surface-exposed outer membrane protein whose expression is regulated in response to environmental temperature and pH. Infect Immun 69:5286–5293. https://doi.org/10.1128/IAI.69.9.5286-5293.2001.
86. Lin YP, Bhowmick R, Coburn J, Leong JM. 2015. Host cell heparan sulfate glycosaminoglycans are ligands for OspF-related proteins of the Lyme disease spirochete. Cell Microbiol 17:1464–1476. https://doi.org/10.1111/cmi.12448.
87. Yamaguchi K, Yu F, Inouye M. 1988. A single amino acid determinant of the membrane localization of lipoproteins in *E. coli*. Cell 53:423–432. https://doi.org/10.1016/0092-8674(88)90162-6.
88. Gennity JM, Inouye M. 1991. The protein sequence responsible for lipoprotein membrane localization in *Escherichia coli* exhibits remarkable specificity. J Biol Chem 266:16458–16464.
89. Lewenza S, Vidal-Ingigliardi D, Pugsley AP. 2006. Direct visualization of red fluorescent lipoproteins indicates conservation of the membrane sorting rules in the family *Enterobacteriaceae*. J Bacteriol 188:3516–3524. https://doi.org/10.1128/JB.188.10.3516-3524.2006.
90. Lewenza S, Mhlanga MM, Pugsley AP. 2008. Novel inner membrane retention signals in *Pseudomonas aeruginosa* lipoproteins. J Bacteriol 190:6119–6125. https://doi.org/10.1128/JB.00603-08.
91. Kumru OS, Schulze RJ, Slusser JG, Zückert WR. 2010. Development and validation of a FACS-based lipoprotein localization screen in the Lyme disease spirochete *Borrelia burgdorferi*. BMC Microbiol 10:277. https://doi.org/10.1186/1471-2180-10-277.
92. Chen S, Kumru OS, Zückert WR. 2011. Determination of *Borrelia* surface lipoprotein anchor topology by surface proteolysis. J Bacteriol 193:6379–6383. https://doi.org/10.1128/JB.05849-11.
93. Chen S, Zückert WR. 2011. Probing the *Borrelia burgdorferi* surface lipoprotein secretion pathway using a conditionally folding protein domain. J Bacteriol 193:6724–6732. https://doi.org/10.1128/JB.06042-11.
94. Kumru OS, Schulze RJ, Rodnin MV, Ladokhin AS, Zückert WR. 2011. Surface localization determinants of *Borrelia* OspC/Vsp family lipoproteins. J Bacteriol 193:2814–2825. https://doi.org/10.1128/JB.00015-11.
95. Lilly AA, Crane JM, Randall LL. 2009. Export chaperone SecB uses one surface of interaction for diverse unfolded polypeptide ligands. Protein Sci 18:1860–1868. https://doi.org/10.1002/pro.197.
96. Liu G, Topping TB, Randall LL. 1989. Physiological role during export for the retardation of folding by the leader peptide of maltose-binding protein. Proc Natl Acad Sci U S A 86:9213–9217. https://doi.org/10.1073/pnas.86.23.9213.
97. Park S, Liu G, Topping T, Cover WH, Randall LL. 1988. Modulation of folding pathways of exported proteins by the leader sequence. Science 239:1033–1035. https://doi.org/10.1126/science.3278378.
98. Randall LL, Hardy SJ. 2002. SecB, one small chaperone in the complex milieu of the cell. Cell Mol Life Sci 59:1617–1623. https://doi.org/10.1007/PL00012488.
99. Zückert WR, Lloyd JE, Stewart PE, Rosa PA, Barbour AG. 2004. Cross-species surface display of functional spirochetal lipoproteins by recombinant *Borrelia burgdorferi*. Infect Immun 72:1463–1469. https://doi.org/10.1128/IAI.72.3.1463-1469.2004.
100. Fraser C, Casjens S, Huang W, Sutton G, Clayton R, Lathigra R, White O, Ketchum K, Dodson R, Hickey E, Gwinn M, Dougherty B, Tomb J, Fleischmann R, Richardson D, Peterson J, Kerlavage A, Quackenbush J, Salzberg S, Hanson M, van Vugt R, Palmer N, Adams M, Gocayne J, Weidman J, Utterback T, Watthey L, McDonald L, Artiach P, Bowman C, Garland S, Fuji C, Cotton M, Horst K, Roberts K, Hatch B, Smith H, Venter J. 1997. Genomic sequence of a Lyme disease spirochaete, *Borrelia burgdorferi*. Nature 390:580–586. https://doi.org/10.1038/37551.
101. Casjens S, Palmer N, van Vugt R, Huang W, Stevenson B, Rosa P, Lathigra R, Sutton G, Peterson J, Dodson R, Haft D, Hickey E, Gwinn M, White O, Fraser CM. 2000. A bacterial genome in flux: the twelve linear and nine circular extrachromosomal DNAs in an infectious isolate of the Lyme disease spirochete *Borrelia burgdorferi*. Mol Microbiol 35:490–516.
102. Notredame C, Higgins DG, Heringa J. 2000. T-Coffee: a novel method for fast and accurate multiple sequence alignment. J Mol Biol 302:205–217. https://doi.org/10.1006/jmbi.2000.4042.
103. Östberg Y, Carroll JA, Pinne M, Krum JG, Rosa P, Bergström S. 2004. Pleiotropic effects of inactivating a carboxyl-terminal protease, CtpA, in *Borrelia burgdorferi*. J Bacteriol 186:2074–2084. https://doi.org/10.1128/JB.186.7.2074-2084.2004.
104. Kumru OS, Bunikis I, Sorokina I, Bergström S, Zückert WR. 2011. Specificity and role of the *Borrelia burgdorferi* CtpA protease in outer membrane protein processing. J Bacteriol 193:5759–5765. https://doi.org/10.1128/JB.05622-11.
105. Lin Y-P, Chen Q, Ritchie JA, Dufour NP, Fischer JR, Coburn J, Leong JM. 2015. Glycosaminoglycan binding by *Borrelia burgdorferi* adhesin BBK32 specifically and uniquely promotes joint colonization. Cell Microbiol 17:860–875. https://doi.org/10.1111/cmi.12407.
106. Skare JT, Shang ES, Foley DM, Blanco DR, Champion CI, Mirzabekov T, Sokolov Y, Kagan BL, Miller JN, Lovett MA. 1995. Virulent strain associated outer membrane proteins of *Borrelia burgdorferi*. J Clin Invest 96:2380–2392. https://doi.org/10.1172/JCI118295.
107. Carroll JA. 2010. Methods of identifying membrane proteins in spirochetes. Curr Protoc Microbiol Chapter 12:Unit12C.2. https://doi.org/10.1002/9780471729259.mc12c02s16.
108. Bunikis J, Noppa L, Ostberg Y, Barbour AG, Bergström S. 1996. Surface exposure and species specificity of an immunoreactive domain of a 66-kilodalton outer membrane protein (P66) of the *Borrelia* spp. that cause Lyme disease. Infect Immun 64:5111–5116.
109. Elias AF, Stewart PE, Grimm D, Caimano M, Eggers CH, Tilly K, Bono JL, Akins D, Radolf JD, Schwan TG, Rosa P. 2002. Clonal polymorphism of *Borrelia burgdorferi* strain B31 MI: implications for mutagenesis in an infectious strain background. Infect Immun 70:2139–2150. https://doi.org/10.1128/IAI.70.4.2139-2150.2002.
110. Florens L, Washburn MP. 2006. Proteomic analysis by multidimensional protein identification technology. Methods Mol Biol 328:159–175.
111. Bunikis I, Kutschan-Bunikis S, Bonde M, Bergström S. 2011. Multiplex PCR as a tool for validating plasmid content of *Borrelia burgdorferi*. J Microbiol Methods 86:243–247. https://doi.org/10.1016/j.mimet.2011.05.004.
112. Zhang Y, Wen Z, Washburn MP, Florens L. 2010. Refinements to label free proteome quantitation: how to deal with peptides shared by multiple proteins. Anal Chem 82:2272–2281. https://doi.org/10.1021/ac9023999.
113. Kariu T, Yang X, Marks CB, Zhang X, Pal U. 2013. Proteolysis of BB0323 results in two polypeptides that impact physiologic and infectious phenotypes in *Borrelia burgdorferi*. Mol Microbiol 88:510–522. https://doi.org/10.1111/mmi.12202.
114. Dunn JP, Kenedy MR, Iqbal H, Akins DR. 2015. Characterization of the beta-barrel assembly machine accessory lipoproteins from *Borrelia burgdorferi*. BMC Microbiol 15:70. https://doi.org/10.1186/s12866-015-0411-y.
115. Howe TR, Mayer LW, Barbour AG. 1985. A single recombinant plasmid expressing two major outer surface proteins of the Lyme disease spirochete. Science 227:645–646. https://doi.org/10.1126/science.3969554.
116. Schwan TG, Burgdorfer W, Garon CF. 1988. Changes in infectivity and plasmid profile of the Lyme disease spirochete, *Borrelia burgdorferi*, as a result of *in vitro* cultivation. Infect Immun 56:1831–1836.

117. Labandeira-Rey M, Skare JT. 2001. Decreased infectivity in *Borrelia burgdorferi* strain B31 is associated with loss of linear plasmid 25 or 28-1. Infect Immun 69:446–455. https://doi.org/10.1128/IAI.69.1.446-455.2001.
118. Purser JE, Norris SJ. 2000. Correlation between plasmid content and infectivity in *Borrelia burgdorferi*. Proc Natl Acad Sci U S A 97:13865–13870. https://doi.org/10.1073/pnas.97.25.13865.
119. Lin T, Gao L, Zhang C, Odeh E, Jacobs MB, Coutte L, Chaconas G, Philipp MT, Norris SJ. 2012. Analysis of an ordered, comprehensive STM mutant library in infectious *Borrelia burgdorferi*: insights into the genes required for mouse infectivity. PLoS One 7:e47532. https://doi.org/10.1371/journal.pone.0047532.
120. Stevenson B, Zückert WR, Akins DR. 2000. Repetition, conservation, and variation: the multiple cp32 plasmids of *Borrelia* species. J Mol Microbiol Biotechnol 2:411–422.
121. Zückert WR, Meyer J. 1996. Circular and linear plasmids of Lyme disease spirochetes have extensive homology: Characterization of a repeated DNA element. J Bacteriol 178:2287–2298. https://doi.org/10.1128/jb.178.8.2287-2298.1996.
122. Eggers CH, Kimmel BJ, Bono JL, Elias AF, Rosa P, Samuels DS. 2001. Transduction by phiBB-1, a bacteriophage of *Borrelia burgdorferi*. J Bacteriol 183:4771–4778. https://doi.org/10.1128/JB.183.16.4771-4778.2001.
123. Alva V, Nam SZ, Soding J, Lupas AN. 2016. The MPI bioinformatics Toolkit as an integrative platform for advanced protein sequence and structure analysis. Nucleic Acids Res 44:W410–W415. https://doi.org/10.1093/nar/gkw348.
124. Revel AT, Blevins JS, Almazan C, Neil L, Kocan KM, de la Fuente J, Hagman KE, Norgard MV. 2005. *bptA* (*bbe16*) is essential for the persistence of the Lyme disease spirochete, *Borrelia burgdorferi*, in its natural tick vector. Proc Natl Acad Sci U S A 102:6972–6977. https://doi.org/10.1073/pnas.0502565102.
125. Barbour AG, Jasinskas A, Kayala MA, Davies DH, Steere AC, Baldi P, Felgner PL. 2008. A genome-wide proteome array reveals a limited set of immunogens in natural infections of humans and white-footed mice with *Borrelia burgdorferi*. Infect Immun 76:3374–3389. https://doi.org/10.1128/IAI.00048-08.
126. Iyer R, Caimano MJ, Luthra A, Axline D, Jr, Corona A, Iacobas DA, Radolf JD, Schwartz I. 2015. Stage-specific global alterations in the transcriptomes of Lyme disease spirochetes during tick feeding and following mammalian host adaptation. Mol Microbiol 95:509–538. https://doi.org/10.1111/mmi.12882.
127. Nigrovic LE, Thompson KM. 2007. The Lyme vaccine: a cautionary tale. Epidemiol Infect 135:1–8. https://doi.org/10.1017/S0950268806007096.
128. Fikrig E, Barthold SW, Marcantonio N, Deponte K, Kantor FS, Flavell RA. 1992. Roles of OspA, OspB, and flagellin in protective immunity to Lyme borreliosis in laboratory mice. Infect Immun 60:657–661.
129. Gilmore RD, Jr, Kappel KJ, Dolan MC, Burkot TR, Johnson BJB. 1996. Outer surface protein C (OspC), but not P39, is a protective immunogen against a tick-transmitted Borrelia burgdorferi challenge–evidence for a conformational protective epitope in OspC. Infect Immun 64:2234–2239.
130. Hellwage J, Meri T, Heikkila T, Alitalo A, Panelius J, Lahdenne P, Seppala IJ, Meri S. 2001. The complement regulator factor H binds to the surface protein OspE of *Borrelia burgdorferi*. J Biol Chem 276:8427–8435. https://doi.org/10.1074/jbc.M007994200.
131. Promnares K, Kumar M, Shroder DY, Zhang X, Anderson JF, Pal U. 2009. *Borrelia burgdorferi* small lipoprotein Lp6.6 is a member of multiple protein complexes in the outer membrane and facilitates pathogen transmission from ticks to mice. Mol Microbiol 74:112–125. https://doi.org/10.1111/j.1365-2958.2009.06853.x.
132. Wada R, Matsuyama S, Tokuda H. 2004. Targeted mutagenesis of five conserved tryptophan residues of LolB involved in membrane localization of *Escherichia coli* lipoproteins. Biochem Biophys Res Commun 323:1069–1074. https://doi.org/10.1016/j.bbrc.2004.08.200.
133. Konovalova A, Silhavy TJ. 2015. Outer membrane lipoprotein biogenesis: Lol is not the end. Philos Trans R Soc Lond B Biol Sci 370:pii=20150030. https://doi.org/10.1098/rstb.2015.0030.
134. Lenhart TR, Akins DR. 2010. *Borrelia burgdorferi* locus BB0795 encodes a BamA orthologue required for growth and efficient localization of outer membrane proteins. Mol Microbiol 75:692–709. https://doi.org/10.1111/j.1365-2958.2009.07015.x.
135. Iqbal H, Kenedy MR, Lybecker M, Akins DR. 2016. The TamB ortholog of *Borrelia burgdorferi* interacts with the beta-barrel assembly machine (BAM) complex protein BamA. Mol Microbiol 102:757–774. https://doi.org/10.1111/mmi.13492.
136. Scoles GA, Papero M, Beati L, Fish D. 2001. A relapsing fever group spirochete transmitted by *Ixodes scapularis* ticks. Vector Borne Zoonotic Dis 1:21–34. https://doi.org/10.1089/153036601750137624.
137. Fukunaga M, Takahashi Y, Tsuruta Y, Matsushita O, Ralph D, McClelland M, Nakao M. 1995. Genetic and phenotypic analysis of *Borrelia miyamotoi* sp. nov., isolated from the ixodid tick *Ixodes persulcatus*, the vector for Lyme disease in Japan. Int J Syst Bacteriol 45:804–810. https://doi.org/10.1099/00207713-45-4-804.
138. Kingry LC, Batra D, Replogle A, Rowe LA, Pritt BS, Petersen JM. 2016. Whole genome sequence and comparative genomics of the novel Lyme borreliosis causing pathogen, *Borrelia mayonii*. PLoS One 11:e0168994. https://doi.org/10.1371/journal.pone.0168994.
139. Pritt BS, Respicio-Kingry LB, Sloan LM, Schriefer ME, Replogle AJ, Bjork J, Liu G, Kingry LC, Mead PS, Neitzel DF, Schiffman E, Hoang Johnson DK, Davis JP, Paskewitz SM, Boxrud D, Deedon A, Lee X, Miller TK, Feist MA, Steward CR, Theel ES, Patel R, Irish CL, Petersen JM. 2016. *Borrelia mayonii* sp. nov., a member of the *Borrelia burgdorferi sensu lato* complex, detected in patients and ticks in the upper midwestern United States. Int J Syst Evol Microbiol 66:4878–4880. https://doi.org/10.1099/ijsem.0.001445.
140. Babb K, McAlister J, Miller J, Stevenson B. 2004. Molecular characterization of *Borrelia burgdorferi erp* promoter/operator elements. J Bacteriol 186:2745–2756. https://doi.org/10.1128/JB.186.9.2745-2756.2004.
141. Barbour AG. 1984. Isolation and cultivation of Lyme disease spirochetes. Yale J Biol Med 57:521–525.
142. Zückert WR. 2007. Laboratory maintenance of *Borrelia burgdorferi*. Curr Protoc Microbiol Chapter 12:Unit 12C.1. https://doi.org/10.1002/9780471729259.mc12c01s4.
143. Zhang JR, Hardham JM, Barbour AG, Norris SJ. 1997. Antigenic variation in Lyme disease borreliae by promiscuous recombination of VMP-like sequence cassettes. Cell 89:275–285. https://doi.org/10.1016/S0092-8674(00)80206-8.
144. Stewart PE, Thalken R, Bono JL, Rosa P. 2001. Isolation of a circular plasmid region sufficient for autonomous replication and transformation of infectious *Borrelia burgdorferi*. Mol Microbiol 39:714–721. https://doi.org/10.1046/j.1365-2958.2001.02256.x.
145. Samuels DS. 1995. Electrotransformation of the spirochete *Borrelia burgdorferi*. Methods Mol Biol 47:253–259.
146. Bunikis J, Barbour AG. 1999. Access of antibody or trypsin to an integral outer membrane protein (P66) of *Borrelia burgdorferi* is hindered by Osp lipoproteins. Infect Immun 67:2874–2883.
147. Ebeling W, Hennrich N, Klockow M, Metz H, Orth HD, Lang H. 1974. Proteinase K from *Tritirachium album* limber. Eur J Biochem 47:91–97. https://doi.org/10.1111/j.1432-1033.1974.tb03671.x.
148. Sweeney PJ, Walker JM. 1993. Proteinase K (EC 3.4.21.14). Methods Mol Biol 16:305–311.
149. Laemmli UK. 1970. Cleavage of structural proteins during the assembly of the head of bacteriophage T4. Nature 227:680–685. https://doi.org/10.1038/227680a0.
150. Barbour AG, Hayes SF, Heiland RA, Schrumpf ME, Tessier SL. 1986. A *Borrelia*-specific monoclonal antibody binds to a flagellar epitope. Infect Immun 52:549–554.
151. Bono JL, Tilly K, Stevenson B, Hogan D, Rosa P. 1998. Oligopeptide permease in *Borrelia burgdorferi*: putative peptide-binding components encoded by both chromosomal and plasmid loci. Microbiology 144 1033–1044.
152. Washburn MP, Wolters D, Yates JR, III. 2001. Large-scale analysis of the yeast proteome by multidimensional protein identification technology. Nat Biotechnol 19:242–247. https://doi.org/10.1038/85686.
153. Pérez-Bercoff A, Koch J, Burglin TR. 2006. LogoBar: bar graph visualization of protein logos with gaps. Bioinformatics 22:112–114. https://doi.org/10.1093/bioinformatics/bti761.